Journal Name

ARTICLE

Ultra-high molecular weight elastomeric polyethylene using an electronically and sterically enhanced nickel catalyst

Received 00th January 20xx,
Accepted 00th January 20xx

DOI: 10.1039/x0xx00000x

www.rsc.org/

Qaiser Mahmood,[a,b] Yanning Zeng,[a] Erlin Yue,[a] Gregory A. Solan,[a,c,*] Tongling Liang [a] and Wen-Hua Sun[a,b,d,*]

A collection of ten related 1,2-bis(imino)acenaphthene-nickel(II) halide complexes, [1-[2,6-{$(C_6H_5)_2CH$}$_2$-4-{*t*-$C(CH_3)_3$}-C_6H_2N]-2-(ArN)$C_2C_{10}H_6$]NiX_2 (X = Br: Ar = 2,6-$Me_2C_6H_3$ **Ni1**, 2,6-$Et_2C_6H_3$ **Ni2**, 2,6-$^iPr_2C_6H_3$ **Ni3**, 2,4,6-$Me_3C_6H_2$ **Ni4**, 2,6-Et_2-4-MeC_6H_2 **Ni5**) and (X = Cl: Ar = 2,6-$Me_2C_6H_3$ **Ni6**, 2,6-$Et_2C_6H_3$ **Ni7**, 2,6-$^iPr_2C_6H_3$ **Ni8**, 2,4,6-$Me_3C_6H_2$ **Ni9**, 2,6-Et_2-4-MeC_6H_2 **Ni10**), each bearing one sterically and electronically enhanced N-2,6-dibenzhydryl-4-t-butylphenyl group, have been prepared and fully characterized. The unsymmetrical nature of the chelating bis(imino)acenaphthene is confirmed in the paramagnetic ^{1}H NMR spectra for **Ni1 - Ni10**, while the molecular structures of **Ni1**, **Ni2** and **Ni6** highlight the unequal steric protection of the nickel center imposed by their respective N,N-ligands. On activation with either Et_2AlCl or MMAO, all the nickel complexes were highly active catalysts in ethylene polymerization [as high as 1.26×10^7 g of PE (mol of Ni)$^{-1}$ h^{-1}] affording exceptionally high molecular weight (up to 3.1×10^6 g mol^{-1}) hyper-branched polyethylene. Analysis of the mechanical properties reveals the ultra-high molecular weight polymers possess high tensile strength, excellent shape fixity and elastic recovery (up to 69%) as well as high elongation at break (ε_b = 843.9%); such materials offer a promising alternative to current thermoplastic elastomers (TPEs).

Introduction

Thermoplastic elastomers (TPEs) combine the processing and recyclable characteristics of thermoplastics with the flexibility and ductility of elastomers. These highly sought after properties give them a key advantage over classical vulcanized rubbers[1] and as a result they have found widespread applications in the electronics, automotive, hose and clothing industries.[2,3] Some examples of TPEs based on block co-polymers include miktoarm block, star-like block, regioirregular block and hyperblock co-polymers. On the other hand, a wide variety of TPEs involving graft co-polymers have been disclosed such as comb-, arborescent-, centipedes-like and multi-graft co-polymers. However, one drawback of these types of TPE relates to the complexity of the routes used to prepare them, often involving multiple steps which in turn raises the price of the end-product.[4] As a more cost-effective and industrially promising strategy, TPEs can be prepared via chain-shuttling ethylene/1-olefin co-polymerization using an early transition metal catalyst.[5,6] Even more coveniently, late transition metal α-diimino-Ni^{+2} (**A,** Chart 1) and -Pd^{+2} pre-catalysts have been shown to generate hyperbranched polyethylenes, properties characteristic of TPEs, using ethylene as the single feed in the polymerization.[7,8] For example, the unsymmetrical 1,2-bis(imino)acenaphthene-nickel(II) halide, $\mathbf{B}_{CHPh2}$ (Chart 1), was found to promote the formation of elastomeric polymers displaying moderately high molecular weight (M_w = 0.17 – 8.7 × 10^5 g mol^{-1}) as well as high elastic recovery and elongation at break.[8l] However, one major

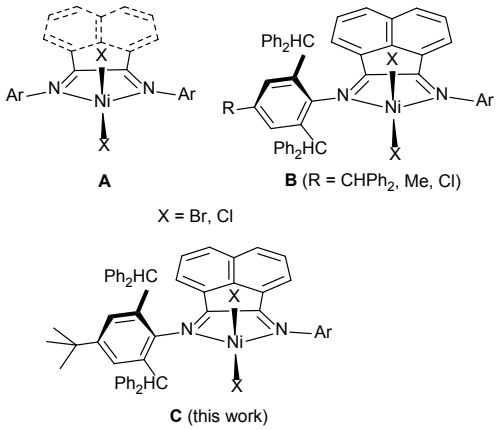

Chart 1. Structural variations in 1,2-bis(imino)acenaphthene-nickel halide pre-catalysts (**A – C**).

[a] *Key Laboratory of Engineering Plastics and Beijing National Laboratory for Molecular Sciences, Institute of Chemistry, Chinese Academy of Sciences, Beijing 100190, China. E-mail. whsun@iccas.ac.cn; Fax: +86-10-62618239; Tel: +86-10-62557955*
[b] *CAS Research/Education Center for Excellence in Molecular Sciences and International School, University of Chinese Academy of Sciences, Beijing 100049, China*
[c] *Department of Chemistry, University of Leicester, University Road, Leicester LE1 7RH, UK*
[d] *State Key Laboratory for Oxo Synthesis and Selective Oxidation, Lanzhou Institute of Chemical Physics, Chinese Academy of Sciences, Lanzhou 730000, China*
Electronic Supplementary Information (ESI) available: X-ray crystallographic data. CCDC 1553630 (**Ni1**), 1553631 (**Ni2**), 1553632 (**Ni6**). For ESI and crystallographic data in CIF or other electronic format see DOI: 10.1039/x0xx00000x

requirement for a practical application of these new materials is a molecular weight high enough to ensure satisfying tensile and elastic properties below and above room temperature.[9] Therefore, there is a drive to find simple and efficient catalysts that are capable of mediating the formation of high or even ultra-high molecular weight TPEs.

As part of our on-going study into exploring correlations between ligand structure and polymer properties/catalytic performance, we have found the benzhydryl-substituted family of 1,2-bis(arylimino)acenaphthene-nickel(II) halide pre-catalysts, **B** (Chart 1),[10] as particularly fruitful. The presence of the two sterically demanding *ortho*-substituted $CHPh_2$ groups on one side of the complex has the effect of not only influencing the temperature stability of the catalyst, but also the catalytic activity, the molecular weight and the degree of branching.[11,12] At the same time, the second N-aryl group can be systematically modified by varying its own steric and electronically properties thereby offering a means of fine tuning the performance of the catalyst. However, too much steric hindrance imposed by this group can, to some degree, compromise the catalytic activity.[13] More recently, we have noticed that the nature of the 4-R substituent on the N-2,6-dibenzhydryl-4-R-phenyl group exerts a further powerful influence on the catalyst performance and polymer microstructure;[14] effects on solubility present an additional outcome.[15] For instance, when R = Me ($\mathbf{B}_{Me}$, Chart 1)[10a] the catalysts exhibit notably higher activity than when R = $CHPh_2$ ($\mathbf{B}_{CHPh2}$, Chart 1),[8l] while the molecular weights are slightly lower and the branching contents show some variation (125 – 337 per 1000 carbon atoms). It is tempting to ascribe these effects to the electron donating properties of the 4-R group, however, rather counterintuitively use of the more electron withdrawing R = Cl ($\mathbf{B}_{Cl}$, Chart 1), leads to even higher activity and molecular weight.[10b]

With a view to further probing the type of 4-R substituent, we target herein the t-Bu member of this family of pre-catalysts, in which an increased positive inductive effect would be anticipated (**C**, Chart 1). The steric and electronic properties of the second aryl group will be modulated and two types of halide ligand (Br, Cl) will be introduced. An in-depth ethylene homo-polymerization study will be performed on the resulting nickel complexes to ascertain the effects on polymer properties (M_w, M_w/M_n, T_m) and catalytic efficiency; the branching content and mechanical properties of the polymers will be thoroughly investigated. Full characterization details for both the ligand and complexes will also be presented.

Results and discussion

Synthesis and characterization

The bis(arylimino)acenaphthenes, 1-[2,6-{$(C_6H_5)_2CH$}$_2$-4-{*t*-$C(CH_3)_3$}-C_6H_2N]-2-(ArN)$C_2C_{10}H_6$ (Ar = 2,6-$Me_2C_6H_3$ **L1**, 2,6-$Et_2C_6H_3$ **L2**, 2,6-^{i}Pr$_2C_6H_3$ **L3**, 2,4,6-$Me_3C_6H_2$ **L4**, 2,6-Et_2-4-MeC_6H_2 **L5**), have been prepared in moderate to good yield by the reaction of 2-(2,6-dibenzhydryl-4-*t*-butylphenylimino)acenaphthylen-1-one (**1**) with the corresponding aniline in toluene at reflux (Scheme 1). Imine-ketone **1** is not commercially available and can be prepared in good yield by the Schiff base condensation reaction of acenaphthylene-1,2-dione with one equivalent of 2,6-dibenzhydryl-4-*t*-butylaniline at room temperature.[16,17] Compounds **L1 – L5** have been characterized by ^{1}H, ^{13}C NMR, FT-IR spectroscopy and by elemental analysis. Treatment of **L1 – L5** with either (DME)$NiBr_2$ (DME = 1,2-dimethoxyethane) in dichloromethane or $NiCl_2{\cdot}6H_2O$ in a mixture of dichloromethane and ethanol gave the corresponding nickel complexes [1-[2,6-{$(C_6H_5)_2CH$}$_2$-4-{*t*-$C(CH_3)_3$}-C_6H_2N]-2-(ArN)$C_2C_{10}H_6$]$NiBr_2$ (Ar = 2,6-$Me_2C_6H_3$ **Ni1**, 2,6-$Et_2C_6H_3$ **Ni2**, 2,6-^{i}Pr$_2C_6H_3$ **Ni3**, 2,4,6-$Me_3C_6H_2$ **Ni4**, 2,6-Et_2-4-MeC_6H_2 **Ni5**) and [1-[2,6-{$(C_6H_5)_2CH$}$_2$-4-{*t*-$C(CH_3)_3$}-C_6H_2N]-2-(ArN)$C_2C_{10}H_6$]$NiCl_2$ (Ar = 2,6-$Me_2C_6H_3$ **Ni6**, 2,6-$Et_2C_6H_3$ **Ni7**, 2,6-^{i}Pr$_2C_6H_3$ **Ni8**, 2,4,6-$Me_3C_6H_2$ **Ni9**, 2,6-Et_2-4-MeC_6H_2 **Ni10**), in good yield, respectively (Scheme 1). Complexes **Ni1 – Ni10** have been characterized by FT-IR, ^{1}H NMR spectroscopy and elemental analysis, while crystals of **Ni1**, **Ni2** and **Ni6** have been the subject of single crystal X-ray diffraction studies. X-ray photoelectron spectroscopic (XPS) data is also reported for all complexes and ligands.

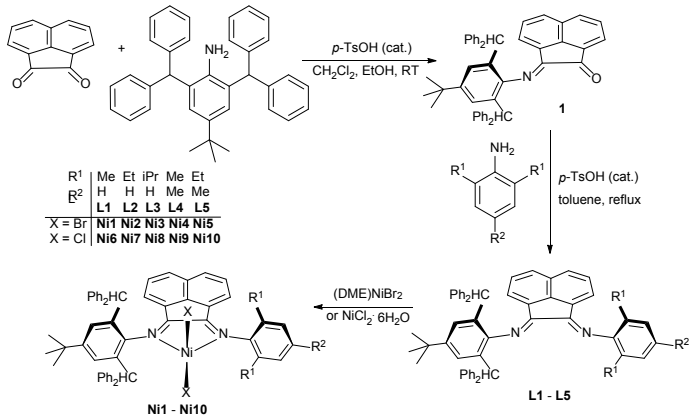

R^1	Me	Et	iPr	Me	Et
R^2	H	H	H	Me	Me
	L1	L2	L3	L4	L5
X = Br	Ni1	Ni2	Ni3	Ni4	Ni5
X = Cl	Ni6	Ni7	Ni8	Ni9	Ni10

Scheme 1. Synthesis of **L1** – **L5** and their complexes **Ni1** – **Ni10**.

Single crystals of **Ni1**, **Ni2** and **Ni6** suitable for the X-ray determination were grown by either layering heptane (**Ni1** and **Ni2**) or by slow diffusion of diethyl ether (**Ni6**) onto their respective dichloromethane solutions. Views of the three structures are shown in Figures 1, 2 and 3; selected bond lengths and angles are compiled in Table 1. The structures are similar and will be discussed together. Each structure consists of a single nickel center surrounded by two halides ligands [Br (**Ni1** and **Ni2**); Cl (**Ni6**)] and two nitrogen atoms belonging to the N,N-chelating bis(imino)acenaphthene (**L1** for **Ni1** and **Ni6**; **L2** for **Ni2**) so as to form a geometry that can be best described as distorted tetrahedral. The N(1)–Ni(1)–N(2) bite angles in each complex are similar at 82.65(8)^o (**Ni1**), 83.04(14)° (**Ni2**) and 82.31(10)° (**Ni6**) and highlight the distortion imposed by the chelating ligand on the geometry. The result is that the X(1)–Ni(1)–X(2) angles are more open at 123.50(3)° (**Ni1**), 123.57(4)° (**Ni2**) and 127.09(5)° (**Ni6**). There is some modest variation in the nickel-nitrogen bond lengths in each complex

with the N1-Ni1 distances in **Ni1** and **Ni6** [2.042(2) Å (**Ni1**), 2.055(3) Å (**Ni6**)] longer than those involving N(2)-Ni(1) [2.023(2) Å (**Ni1**), 2.023(3) Å (**Ni6**)], reflecting the presence of the more bulky N-2,6-dibenzhydryl-4-*t*-butylphenyl group on N1. Surprisingly this is not mirrored in **Ni2** with the corresponding distances statistically comparable [N1-Ni1 2.039(3) Å *vs.* 2.047(4) Å]. The range in imine bond lengths of 1.283(3) – 1.300(5) Å for all three complexes is typical of that expected for this functional group.[12] In addition, the imine-vectors are essentially co-planar with the adjacent acenaphthene unit whereas the plane of the N-2,6-dibenzhydryl-4-*t*-butylphenyl rings are inclined close to perpendicular with regard to the chelate ring plane. Conversely, the inclination of the second N-aryl group (aryl = 2,6-$Me_2C_6H_3$ **Ni1, Ni6;** 2,6-$Et_2C_6H_3$ **Ni2**) reveals some variation [83.2° **Ni1**, 86.4° **Ni2**, 86.3° **Ni6**]. Related structures containing unsymmetrical bis(imino)acenaphthenes have been previously reported and indeed **Ni1**, **Ni2** and **Ni6** display similar features.[12,18]

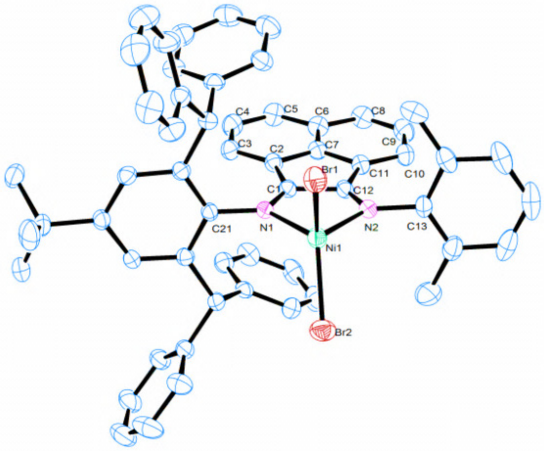

Figure 1. ORTEP representation of **Ni1** with thermal ellipsoids set at 50% probability level; all hydrogen atoms are omitted for clarity.

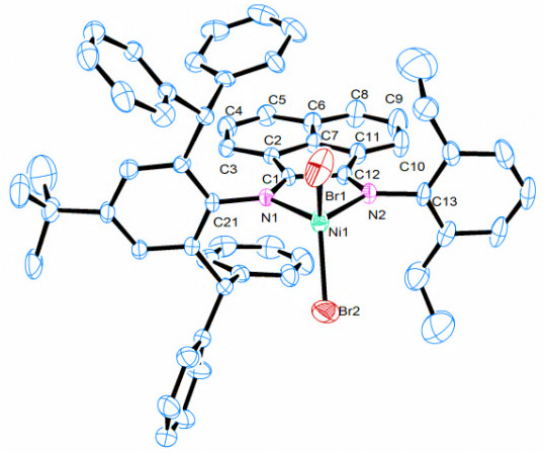

Figure 2. ORTEP representation of **Ni2** with thermal ellipsoids set at 50% probability level; all hydrogen atoms are omitted for clarity.

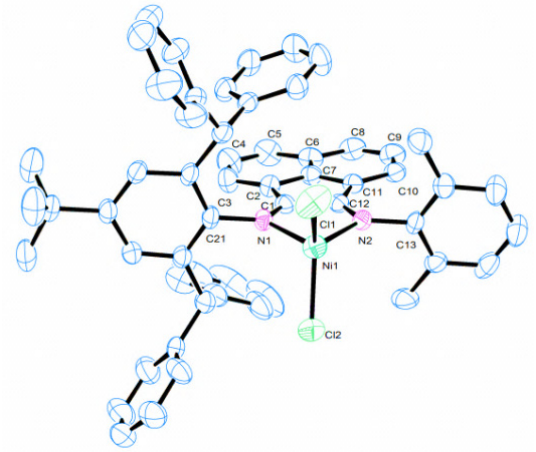

Figure 3. ORTEP representation of **Ni6** with thermal ellipsoids set at 50% probability level; all hydrogen atoms are omitted for clarity.

In the IR spectra, **Ni1** – **Ni10** display ν(C=N)$_{imine}$ stretching vibrations in the range 1616 – 1655 cm^{-1} which are typically *ca.* 20 cm^{-1} lower in wavenumber than that observed in their free ligands. Such a shift is consistent with the effective coordination between the N,N-ligand and the metal center.[10] Broad paramagnetically shifted peaks are a feature of the ^{1}H NMR spectra [recorded in deuterated dichloromethane (CD_2Cl_2) at ambient temperature] of all the complexes and peak assignment has been made through a comparison with data recorded for related Ni(II) (S = 1) complexes.[8l,19] Due to the unsymmetrical nature of the acenaphthene unit, each complex features six distinct singlets for this group in their ^{1}H NMR spectra all integrating to one proton in the range δ +4.5 to +28 (see SI). In addition, a prominent singlet for the *t*-butyl protons is evident at *ca.* δ 3.71 in the ^{1}H NMR spectra for the nickel bromides (**Ni1 – Ni5**), while for the nickel chlorides (**Ni6 – Ni10**) this resonance is shifted slightly downfield to *ca.* δ 4.54. The microanalytical data are supportive of the elemental compositions proposed.

Table 1 Selected bond lengths (Å) and angles (°) for **Ni1**, **Ni2** and **Ni6**

	Ni1	**Ni2**	**Ni6**
X	Br	Br	Cl
Bond lengths (Å)			
Ni(1)–X(1)	2.3430(8)	2.3379(10)	2.1901(11)
Ni(1)–X(2)	2.3368(7)	2.3350(9)	2.2177(11)
Ni(1)–N(1)	2.042(2)	2.039(3)	2.055(3)
Ni(1)–N(2)	2.023(2)	2.047(4)	2.023(3)
N(1)–C(1)	1.283(3)	1.300(5)	1.288(4)
N(1)–C(21)	1.442(3)	1.440(5)	1.445(4)
N(2)–C(12)	1.283(3)	1.290(6)	1.274(4)
N(2)–C(13)	1.440(3)	1.452(5)	1.443(4)
Angles (°)			
X(1)–Ni(1)–X(2)	123.50(3)	123.57(4)	127.09(5)
N(1)–Ni(1)–N(2)	82.65(8)	83.04(14)	82.31(10)
N(1)–Ni(1)–X(1)	107.52(6)	111.25(11)	110.60(8)
N(1)–Ni(1)–X(2)	115.66(5)	111.37(11)	105.06(8)
N(2)–Ni(1)–X(1)	108.37(6)	111.08(12)	113.94(8)
N(2)–Ni(1)–X(2)	111.58(6)	109.20(12)	108.38(8)

X-ray photoelectron spectroscopic (XPS) measurements were also carried out for all the ligands (**L1** – **L5**) and nickel complexes (**Ni1** – **Ni10**) to probe the binding energies of the nickel and nitrogen atoms. The binding energies for the regions relating to the N (1s) and Ni (2p) levels are given in Table S1; the N (1s) core level spectra for representative **L2** and its corresponding nickel bromide and chloride complexes (**Ni2** and **Ni7**) are shown in Figure S1. The enhanced energies of the N (1s) level for **Ni2** and **Ni6** with respect to free **L2** are consistent with the coordination of the imine nitrogen with the metal center [399.72 eV (**Ni2**) and 399.79 eV (**Ni7**) *vs.* 399.38 eV (**L2**)].[12i,15] Furthermore, the binding energies of the N (1s) level in the case of two bromide nickel complexes (**Ni1** and **Ni2**) show a discernable increase when compared with their nickel chloride counterparts (**Ni6** and **Ni7**). It is assumed that the more electron-withdrawing chloride group indirectly reduces the electron density on the imine nitrogen. Surprisingly, the inverse trend is observed for the remaining nickel complexes (*cf.* **Ni3** *vs.* **Ni8, Ni4** *vs.* **Ni9** and **Ni5** *vs.* **Ni10**, see SI). Similar findings have been noted in our previous study.[12i]

Catalytic evaluation for ethylene polymerization

Co-catalyst screen

In order to examine the catalytic potential of the nickel bromide (**Ni1** – **Ni5**) and chloride complexes (**Ni6** – **Ni10**) in ethylene polymerization, preliminary tests were conducted using solely **Ni1** with a range of different aluminum-alkyl co-catalysts, including methylaluminoxane (MAO), modified methylaluminoxane (MMAO), diethylaluminum chloride (Et_2AlCl) and dimethylaluminum chloride (Me_2AlCl). Typically, the tests were performed at 30 °C in toluene under 10 atmospheres of ethylene pressure over a period of 30 minutes; the results of this initial screen are presented in Table 2. Examination of the data, reveals Et_2AlCl displayed by far the highest activity, MMAO next best while Me_2AlCl and MAO fall at the bottom end of the activity range. Meanwhile, the molecular weight of the polymers, as a function of the co-catalyst, increase in the order: Me_2AlCl < Et_2AlCl < MAO < MMAO. It is plausible that the sterically bulky methylaluminoxane counter-ion undergoes slow polymer chain transfer compared to chain propagation according to the olefin-separated ion-pair model.[20] On the basis of the level of catalytic activity, subsequent more in-depth studies focused on the use of MMAO and Et_2AlCl as the co-catalysts.

Table 2 Ethylene polymerization using **Ni1** with a range of different co-catalysts[a]

Entry	Co-cat.	Al/Ni	Yield/g	Activity[b]	M_w[c]	M_w/M_n[c]	T_m[d]/°C
1	MAO	1000	0.55	0.55	6.0	6.1	114.9
2	MMAO	1000	2.26	2.26	9.2	3.0	76.7
3	Me_2AlCl	200	0.31	0.31	0.5	4.0	98.0
4	Et_2AlCl	200	8.58	8.58	2.1	3.7	58.1

[a] General conditions: 2.0 µmol of **Ni1**, 100 mL of toluene, 10 atm. of ethylene, 30 min., 30 °C. [b] x 10^6 g of PE (mol of Ni)$^{-1}$ h^{-1}. [c] M_w: x 10^5 g mol^{-1}, determined by GPC. [d] Determined by DSC.

Screening of Ni1/Et_2AlCl

With the intent to establish the optimal polymerization conditions, a study was initiated to investigate the performance of **Ni1**/Et_2AlCl under various reaction conditions linked to the Al/Ni ratio, reaction temperature and the run time; the results are collected in Table 3.

Changes in the Al/Ni ratio showed noticeable effects on the catalytic activity and properties of the polyethylenes. When the Al/Ni ratio was increased from 200 to 600 and the temperature maintained at 30 °C, the catalytic activity of **Ni1**/Et_2AlCl gradually improved to a maximum of 10.62 × 10^6 g of PE (mol of Ni)$^{-1}$ h^{-1} with the ratio at 600 (entry 3, Table 3). On further increasing the Al/Ni ratio this high activity was found to lower (entries 4 and 5, Table 3). In a similar way the molecular weight of the polyethylene reached its highest value at an Al/Ni ratio of 600 (entry 3, Table 3). Above this value the molecular weight falls, this correlation between Al/Ni ratio and molecular weight is illustrated in the GPC curves shown in Figure S2. It is assumed that the high molar ratio of Al/Ni enhances the rate of chain transfer as compared to chain propagation leading to a high rate of chain termination forming lower molecular weight polyethylene.[21] These findings are consistent with previously reported systems.[12]

To examine the thermal stability of **Ni1**/Et_2AlCl, the polymerization tests were performed over 10 degree increments from 20 to 50 °C with the Al/Ni ratio fixed at 600 (entries 3, 6 – 8, Table 3). A peak in activity was found at 30 °C [10.62 × 10^6 g of PE (mol of Ni)$^{-1}$ h^{-1}] which dropped to almost half at 40 °C and then less dramatically fell to 3.90 × 10^6 g of PE (mol of Ni)$^{-1}$ h^{-1} at 50 °C. Lower activities on increasing the temperature can be attributed to the partial deactivation of the active species at higher temperature,[11i,22] as well as lower solubility of the ethylene monomer in toluene at these temperatures.[23] Similar results have previously been reported for other catalysts bearing benzhydryl-substituted unsymmetrical bis(imino)acenaphthene ligand frames.[12] Meanwhile higher molecular weight polyethylene is evident at lower temperature (Figure 4). At 20 or 30 °C, little difference in

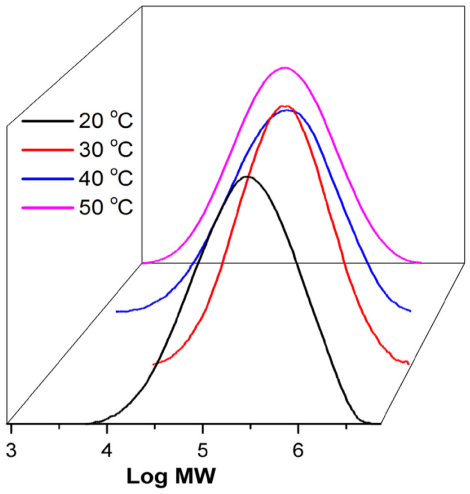

Figure 4. GPC curves of the polyethylenes obtained using **Ni1**/Et_2AlCl at different reaction temperatures (entries 3, 6 – 8 in Table 3).

Table 3. Optimization of the polymerization conditions using **Ni1**/Et_2AlCl[a]

Entry	Temp. (°C)	Time (min.)	Al/Ni	Yield (g)	Activity[b]	M_w[c]	M_w/M_n[c]	T_m[d] (°C)
1	30	30	400	9.15	9.15	2.8	3.3	53.8
2	30	30	500	10.29	10.29	2.8	3.3	55.1
3	30	30	600	10.62	10.62	5.0	3.1	52.5
4	30	30	700	9.75	9.75	2.3	3.8	56.7
5	30	30	800	9.08	9.08	2.3	3.5	53.4
6	20	30	600	5.27	5.27	5.0	3.7	87.1
7	40	30	600	5.72	5.72	2.3	4.9	51.2
8	50	30	600	3.90	3.90	1.0	4.6	29.1
9	30	5	600	2.32	13.97	7.8	2.2	70.0
10	30	10	600	5.42	16.32	8.0	2.0	68.1
11	30	15	600	8.18	16.36	1.9	4.9	48.9
12	30	45	600	12.52	8.34	1.8	4.9	56.3
13	30	60	600	12.60	6.30	2.1	5.0	61.6

[a] General conditions: 2.0 µmol of **Ni1**; 100 mL of toluene for 10 atm. of ethylene. [b] x 10^6 g of PE (mol of Ni)$^{-1}$ h^{-1}. [c] M_w: x 10^5 g mol^{-1}, determined by GPC. [d] Determined by DSC.

molecular weight was observed, however, on further raising the temperature, significantly lower molecular weight polymer was obtained. Again it is presumed that the higher temperature enhances the rate of chain termination with respect to chain propagation resulting in lower molecular weight polyethylene.[24] The melting temperatures (T_m) of the polymers were found to gradually drop on increasing the reaction temperature, highlighting the amorphous nature of the material which relates to the high degree of branching (*vide infra*). Notably this reduction in T_m is slightly more apparent than that seen for the polyethylene generated by previously reported pre-catalysts of the same family (**B**, in Chart 1).[10]

In order to probe the lifetime of **Ni1**/Et_2AlCl at 30 °C, the ethylene polymerization runs were performed over six different reaction times namely 5, 10, 15, 30, 45 and 60 minutes with the Al/Ni molar ratio fixed at 600. The results reveal that the highest activity of 16.36 × 10^6 g of PE (mol of Ni)$^{-1}$ h^{-1} was achieved after 15 minutes (entry 11, Table 3). These results suggest that a short induction period was required to fully generate the active species following addition of the co-catalyst. Beyond that, the activities gradually decreased (entries 3, 12 and 13, Table 3). It is likely that this lowering in activity can be attributed to the partial deactivation of active species over the course of the reaction. Even though the activity drops, it still maintains at a remarkably high level after 1 hour [6.30 × 10^6 g of PE (mol of Ni)$^{-1}$ h^{-1}], indicative of a highly stable active species. Scrutiny of the molecular weights of the resultant polyethylenes showed no clear trend.[11c]

Screening of Ni1/MMAO

In a manner similar to that described for **Ni1**/Et_2AlCl, the reaction conditions were optimized using **Ni1** in combination this time with MMAO as co-catalyst; the results are collected in Table 4. On inspection of the data, the highest activity of 8.30 × 10^6 g of PE (mol of Ni)$^{-1}$ h^{-1} was achieved when the polymerization run was performed at 30 °C with an Al/Ni ratio of 3000 over a 30 minute run time (entry 4, Table 4). In comparison with **Ni1**/Et_2AlCl, lower activities were observed, but the polyethylene showed extremely high molecular weight and narrow polydisperity [4.0 – 12.7 x 10^5 g mol^{-1}; M_w/M_n = 2.1 – 3.3] (Figure S3).

With regard to the thermal stability, **Ni1**/MMAO exhibited its optimal performance at 30 °C [8.30 × 10^6 g of PE (mol of Ni)$^{-1}$ h^{-1}]. On raising the temperature to 40 °C the activity dropped by more than a half [3.12 × 10^6 g of PE (mol of Ni)$^{-1}$ h^{-1}] (entry 8, Table 4); at 50 °C the activity remained essentially constant [3.11 × 10^6 g of PE (mol of Ni)$^{-1}$ h^{-1}] (entry 9, Table 4). As was the case with **Ni1**/Et_2AlCl, the molecular weights and melt temperatures of the polymer (T_m = 47 – 94 °C) gradually decreased with a rise in the temperature (Figure 5).[24]

With the Al/Ni ratio and temperature set at 3000 at 30 °C, respectively, the lifetime of the active species derived from **Ni1**/MMAO was studied. The highest activity of 9.8 × 10^6 g of PE (mol of Ni)$^{-1}$ h^{-1} was noted after a period of 5 minutes (entry 10, Table 4), after which the activities slowly drop over longer reaction times. The molecular weight of the polyethylene appears to decrease after the first 15 minutes

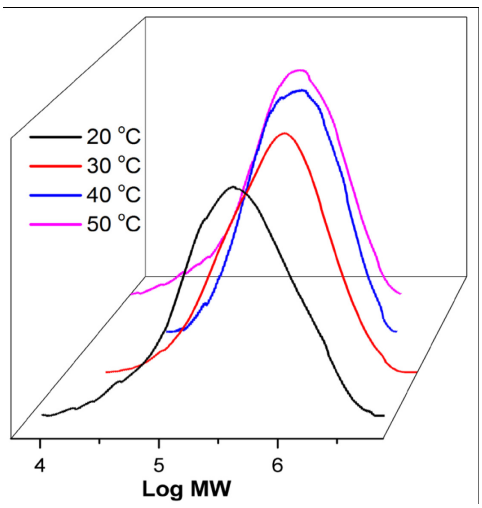

Figure 5. GPC curves of the polyethylenes obtained using **Ni1**/MMAO at different reaction temperatures (entries 4, 7 – 9, Table 4).

Table 4 Optimization of the polymerization conditions using **Ni1**/MMAO[a]

Entry	Temp. (°C)	Time (min.)	Al/Ni	Yield (g)	Activity[b]	M_w[c]	M_w/M_n[c]	T_m[d] (°C)
1	30	30	1500	4.47	4.47	12.7	2.3	74.5
2	30	30	2000	5.58	5.58	4.0	2.9	75.2
3	30	30	2500	6.22	6.22	8.3	2.1	68.8
4	30	30	3000	8.30	8.30	6.4	2.6	63.2
5	30	30	3500	6.10	6.10	7.5	3.2	70.3
6	30	30	4000	5.15	5.15	11.5	2.7	78.9
7	20	30	3000	4.18	4.18	5.4	3.2	94.0
8	40	30	3000	3.12	3.12	5.0	2.0	53.9
9	50	30	3000	3.11	3.11	3.1	2.6	47.0
10	30	5	3000	1.63	9.82	11.8	1.9	77.0
11	30	10	3000	2.76	8.31	9.4	1.8	79.8
12	30	15	3000	4.54	9.08	4.9	2.1	63.4
13	30	45	3000	10.10	6.73	6.9	2.6	68.5
14	30	60	3000	11.05	5.53	8.2	3.1	68.7

[a] General conditions: 2.0 µmol of **Ni1**; 100 mL of toluene for 10 atm. of ethylene. [b] x 10^6 g of PE (mol of Ni)$^{-1}$ h^{-1}. [c] M_w: x 10^5 g mol^{-1}, determined by GPC. [d] Determined by DSC.

(entries 10 - 12, Table 4) and then increase (entries 4, 13, 14, Table 4). This observation can likely be accounted for by the time required for the chain propagation and regeneration of active species following chain transfer.[11c]

Screening of Ni1 – Ni10 with either Et_2AlCl or MMAO

Using the optimized reaction conditions established independently for **Ni1**/Et_2AlCl and **Ni1**/MMAO, all the remaining pre-catalysts (**Ni2 – Ni10**) were additionally evaluated using Et_2AlCl (Table 5) and MMAO (Table 6).

With Et_2AlCl [Al/Ni ratio = 600, 30 °C and 30 minute run time], all the bromide pre-catalysts (**Ni1 – Ni5**) displayed excellent activities in the range 9.5 – 12.57 × 10^6 g of PE (mol of Ni)$^{-1}$ h^{-1} (entries 1 – 5, Table 5) and followed the order: **Ni4** [2,4,6-tri(Me)] > **Ni1** [2,6-di(Me)] > **Ni3** [2,6-di(^{i}Pr)] ~ **Ni2** [2,6-di(Et)] > **Ni5** [2,6-di(Et)-4-Me]. **Ni4** was the standout performer showing the highest activity of 12.57 × 10^6 g of PE (mol of Ni)$^{-1}$ h^{-1} *vs.* 10.62 × 10^6 g of PE (mol of Ni)$^{-1}$ h^{-1} for **Ni1** (entry 4 *vs.* 1, Table 5). Clearly a combination of steric and electronic factors is operational with the least sterically bulky N-aryl groups tending to give the higher activities. Some further correlation with the Ni (2p) binding energies for **Ni4** (856.23 eV) over **Ni1** (855.52 eV) is also possible as relatively high Ni (2p) binding energies indicate low electron density around the nickel center, which when extrapolated to the active catalyst would improve ethylene coordination.[12a,15]

Table 5 Ethylene polymerization using **Ni1** – **Ni10**/Et_2AlCl[a]

Entry	Precat.	Yield (g)	Activity[b]	M_w[c]	M_w/M_n[c]	T_m[d] (°C)
1	**Ni1**	10.62	10.62	5.0	3.1	52.5
2	**Ni2**	10.37	10.37	6.0	2.5	50.7
3	**Ni3**	10.45	10.45	9.0	2.4	51.5
4	**Ni4**	12.57	12.57	4.0	2.7	52.7
5	**Ni5**	9.5	9.50	5.8	2.5	43.1
6	**Ni6**	5.43	5.43	7.3	2.4	62.6
7	**Ni7**	4.42	4.42	9.9	2.3	67.4
8	**Ni8**	4.31	4.31	10.8	2.4	58.8
9	**Ni9**	4.63	4.63	7.2	2.4	54.0
10	**Ni10**	4.52	4.52	10.5	2.3	67.1

[a] General conditions: 2.0 µmol of **Ni**, 100 mL of toluene, 10 atm of ethylene, 30 min, 30 °C and 600 Al/Ni ratio. [b] 10^6 g of PE (mol of Ni)$^{-1}$ h^{-1}. [c] M_w: x 10^5 g mol^{-1}, M_w and M_w/M_n determined by GPC. [d] Determined by DSC.

In comparison with the structurally similar pre-catalysts, [1-[2,6-{$(C_6H_5)_2CH$}$_2$-4-R-C_6H_2N]-2-(ArN)$C_2C_{10}H_6$]$NiBr_2$ (R = Me[10a] ($\mathbf{B}_{Me}$, Chart 1), Cl[10b] ($\mathbf{B}_{Cl}$, Chart 1) and $CHPh_2$[8l] ($\mathbf{B}_{CHPh2}$, Chart 1), the introduction of a *t*-butyl at the *para*-position in **Ni1** – **Ni5** revealed a notable enhancing effect on catalytic activity. This could be due to the positive inductive effect of the *t*-butyl group increasing the stability of the active species in favour of high polymer productivities. On the other hand, the non-polar *t*-butyl group has a noticeable solubilizing effect on the pre-catalyst in the polymerization solvent toluene which could lead to a cleaner activation with the co-catalyst. Significantly, the more sterically hindered **Ni3** afforded very high molecular weight polyethylene [9.0 x 10^5 g mol^{-1}] with narrow polydispersity (M_w/M_n = 2.4) (entry 3, Table 5). Indeed when compared with $\mathbf{B}_{Me}$,[10a] $\mathbf{B}_{Cl}$[10b] and $\mathbf{B}_{CHPh2}$[8l] (Chart 1), **Ni1** – **Ni5** in general, favour the formation of much higher molecular weight polyethylene. It is uncertain as to the origin of this molecular weight increase but it could, in a similar way to the catalytic activity, relate to the electron donating capacity of the *t*-butyl group and in turn its impact on the rate of propagation as compared to chain termination.[11a-c]

By contrast, the catalytic activities of the nickel chlorides, **Ni6** – **Ni10**, with Et_2AlCl as co-catalyst decreased in the order: **Ni6** [2,6-di(Me)] > **Ni9** [2,4,6-tri(Me)] > **Ni10** [2,6-di(Et)-4-Me] > **Ni7** [2,6-di(Et)] > **Ni8** [2,6-di(^{i}Pr)]. Some variations in the order as compared to that seen with **Ni1 – Ni5** but again higher activities are seen for the less sterically bulky pre-catalysts. Generally however, **Ni6 – Ni10**/Et_2AlCl, exhibit lower activities (entries 6-10, Table 5) when put alongside their bromide counterparts. For example chloride **Ni9** gave an activity of 4.63 × 10^6 g of PE (mol of Ni)$^{-1}$ h^{-1} (entry 9, Table 5) which is considerably lower than for the bromide analog **Ni4** [12.57 ×

10^6 g of PE (mol of Ni)$^{-1}$ h^{-1}] (entry 4, Table 5). The precise explanation behind these differences in catalytic performance between chloride and bromide remains unclear but it may relate to the different activation processes, stability of the active species and resultant counter-ion type.[12] As regards the polymers, all the nickel chloride complexes gave high to ultra-high molecular weights [7.2 – 10.8 × 10^5 g mol^{-1}] and melt temperature values that vary in the range 54.0 to 67.4 °C, properties which are slightly higher than those seen for the polyethylenes obtained using the nickel bromide set of pre-catalysts. Once again the more sterically hindered 2,6-diisopropyl pre-catalyst **Ni8**, the chloride analogue of **Ni3**, afforded the highest molecular weight polyethylene of this series [10.8 x 10^5 g mol^{-1}]. Interestingly, **Ni6** – **Ni10**, all showed a very narrow range for their molecular weight distributions (M_w/M_n = 2.3 – 2.4) indicative of single site behavior of the active species.

With MMAO as the co-catalyst, the nickel bromides **Ni1** – **Ni5** [optimal conditions: Al/Ni ratio = 3000, 30 °C and 30 minutes run time] exhibited noticeably lower activities (entries 1-5, Table 6) than that observed with **Ni1** – **Ni5**/Et_2AlCl. However, the properties of the polyethylenes are quite different especially the range in molecular weights which cross quite noticeably into the ultra-high molecular weight window (5.1 – 30.8 × 10^5 g mol^{-1}). In terms of their relative activities, the nickel bromide pre-catalysts decreased in the order: **Ni1** [2,6-di(Me)] > **Ni4** [2,4,6-tri(Me)] > **Ni2** [2,6-di(Et)] > **Ni5** [2,6-di(Et)-4-Me] > **Ni3** [2,6-di(^{i}Pr)]. Similar to shown earlier it is apparent that the least sterically hindered bulky group showed higher activities. As observed with Et_2AlCl, the activities for the chlorides, **Ni6** – **Ni10**, were less than for the bromides, albeit less obviously; the order in activity was: **Ni9** [2,4,6-tri(Me)] > **Ni6** [2,6-di(Me)] > **Ni10** [2,6-di(Et)-4-Me] > **Ni7** [2,6-di(Et)] > **Ni8** [2,6-di(^{i}Pr)]. Dissimilar to the nickel bromide pre-catalysts, the range of activities [3.71 – 5.31 × 10^6 g of PE (mol of Ni)$^{-1}$ h^{-1}] is less pronounced for these nickel chlorides (entries 6-10, Table 6), while the molecular weights observed all fall in the ultra-high molecular weight range (10.4 – 15.5 × 10^5 g mol^{-1}). As with the **Ni1**-**Ni10**/Et_2AlCl-promoted systems, the ones involving MMAO as co-catalyst reveal similar effects on activity and molecular weight. By comparison with previously reported unsymmetrical bis(arylimino)acenaphthene-nickel catalysts,[12,18] it is clear once again that the incorporation of a *para t*-butyl group to the *N*-2,6-benzydrylphenyl unit has a key influence on the productivities as well as the molecular weight of the resultant polyethylene (Figure 6). Indeed, the more sterically hindered **Ni3** pre-catalyst in combination with MMAO gives the highest molecular weight of all the polymers generated in this work [30.8 × 10^5 g mol^{-1}] (entry 3, Table 6), which is higher than seen when Et_2AlCl as the co-catalyst [9.0 x 10^5 g mol^{-1}] (entry 3, Table 5). As already mentioned it would seem likely that the t-Bu group retards chain transfer/termination with respect to chain propagation resulting in this very high molecular weight polyethylene.[12] Furthermore, the even higher molecular weight observed with MMAO as co-catalyst may be due, as alluded to earlier, to the sterically bulky methylaluminoxane counter-anions undergoing slow polymer chain transfer *verses* chain propagation as described by the olefin-separated ion-pair model.[20]

Table 6 Ethylene polymerization using **Ni1** – **Ni10**/MMAO[a]

Entry	Precat.	Yield (g)	Activity[b]	M_w[c]	M_w/M_n[c]	T_m[d] (°C)
1	**Ni1**	8.30	8.30	6.4	2.6	63.2
2	**Ni2**	6.13	6.13	5.1	2.8	60.0
3	**Ni3**	5.88	5.88	30.8	2.4	53.4
4	**Ni4**	8.20	8.20	15.7	1.9	59.0
5	**Ni5**	6.00	6.00	19.8	2.5	63.1
6	**Ni6**	5.12	5.12	15.5	2.1	92.9
7	**Ni7**	3.75	3.75	12.4	2.3	85.2
8	**Ni8**	3.71	3.71	14.3	2.4	72.7
9	**Ni9**	5.31	5.31	10.4	3.1	82.3
10	**Ni10**	4.48	4.48	13.5	2.9	73.6

[a] General conditions: 2.0 µmol of **Ni**, 100 mL of toluene, 10 atm of ethylene, 30 min, 30 °C and 3000 Al/Ni ratio. [b] 10^6 g of PE (mol of Ni)$^{-1}$ h^{-1}. [c] M_w: x 10^5 g mol^{-1}, M_w and M_w/M_n determined by GPC. [d] Determined by DSC.

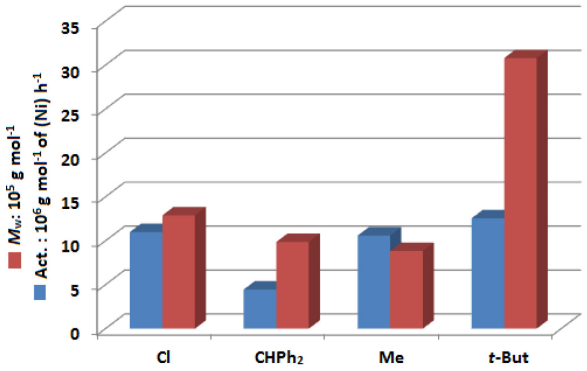

Figure 6. Comparison of the catalytic performance of the current pre-catalysts with previously reported analogues (B_{Me}[10a], B_{Cl},[10b] B_{CHPh2}[8l], see Chart 1).

Microstructure of the Polyethylene

To assess the branching architecture, samples of the polyethylene obtained using **Ni1**/Et_2AlCl at 30 °C (entry 3, Table 3) and **Ni1**/MMAO at 30 and 50 °C (entries 4 and 9, Table 4) were selected as representative examples for high temperature ^{13}C NMR spectroscopy [recorded in deuterated 1,2-dichlorobenzene at 135 °C]; the resulting spectra are shown in Figures 7, 8 and S4, respectively. Using assignments listed in the literature, the branching content and branch type could be readily determined (Table S2 –S4).[25] The polyethylene obtained using **Ni1**/Et_2AlCl at 30 °C possessed 138 branches per 1000 carbons which included methyl (54.7%), ethyl (6.1%), propyl (4.9%), butyl (9.1%), amyl (4.9%), longer chain branches (12%) and 1,6-paired methyl branches (8.3%). Notably, a greater number of branches is observed when compared to previously reported polyethylenes obtained using related pre-catalysts.[11c,12d] For the sample obtained using **Ni1**/MMAO at 30 °C the branching content increased (Figure 8) with 173 branches per 1000 carbons including methyl (52.6%), ethyl (7.0%), butyl (11.5%), longer chain branches (17.6%) and 1,6-paired methyl branches (17.8%). With **Ni1**/MMAO at 50 °C the polyethylene displayed 142 branches per 1000 carbons (Figure

S4). Surprisingly, the latter catalyst yielded polyethylene with a lower number of branches despite an increase in the temperature; an observation that is contrary to that observed elsewhere.[12a,b] Nevertheless, a comparatively high percentage of methyl and ethyl branches was observed at 50 °C.

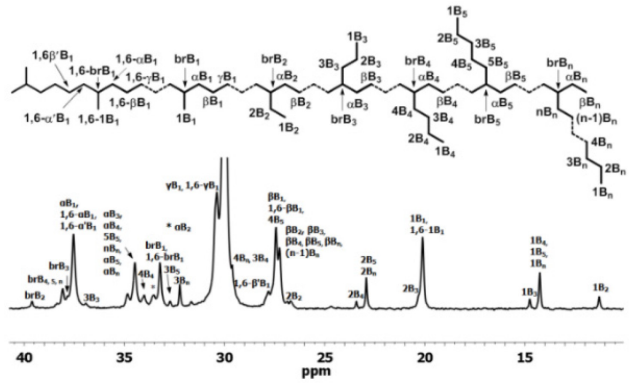

Figure 7. ^{13}C NMR spectrum of the polyethylene obtained using **Ni1**/Et_2AlCl at 30 °C (entry 3, Table 3); recorded in deuterated 1,2-dichlorobenzene at 135 °C

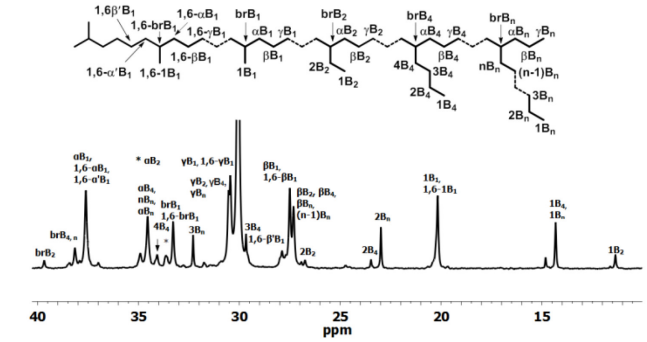

Figure 8. ^{13}C NMR spectrum of the polyethylene obtained using **Ni1**/MMAO at 30 °C (entry 4, Table 4); recorded in deuterated 1,2-dichlorobenzene at 135 °C

Mechanical Properties of the Polyethylene

The mechanical properties of the lower molecular weight polyethylene samples designated PE-$20_{E/Ni1}$, PE-$30_{E/Ni1}$, PE-$40_{E/Ni1}$ and PE-$50_{E/Ni1}$ corresponding to the entries 3, 6-8 in Table 3 in which Et_2AlCl was employed as co-catalyst, were initially studied by stress–strain measurements; the resulting data is presented in Table 7 while stress-strain curves are illustrated in Figure 9.[26] Each mechanical test was performed with five specimens of each material in order to achieve consistent results. Notably, the lowest ultimate tensile stress (3.28 MPa) allied with the highest strain at break (ε_b = 1002%) was observed for PE-$50_{E/Ni1}$, this can be attributed to the material being almost amorphous owing to the high branching content. In comparison with previously reported results obtained with pre-catalyst $\mathbf{B}_{CHPh2}$ (Chart 1),[8l] PE-$50_{E/Ni1}$ gave improved ultimate tensile stress as well as higher elongation at break. It is apparent that the presence of such high elasticity was caused by poor crystallinity, which was in-turn relates to the high branching content. As the crystallinity (X_c) gradually improved in PE-$40_{E/Ni1}$ to 8.9%, the ultimate tensile strength was increased to 5.74 MPa, while the elongation at break decreased to 661.3%. Raising the crystallinity still higher from 10.2 to 11.5% (PE-$30_{E/Ni1}$ to PE-$20_{E/Ni1}$), resulted in the ultimate tensile stress increasing further from 6.11 to 8.52 MPa. In contrast, the elongation at break (ε_b) tends to decrease with increasing crystallinity. In general, the polyethylene displaying the higher branching content showed lower ultimate tensile strength and better elastomeric properties. These observations suggest that the tensile properties of the polyethylene obtained were significantly influenced by the branching architectures and the crystallinity.[27]

Secondly, the corresponding series of polyethylene samples made with MMAO as co-catalyst, PE-$20_{M/Ni1}$, PE-$30_{M/Ni1}$, PE-$40_{M/Ni1}$ and PE-$50_{M/Ni1}$ (entries 4, 7-9 in Table 4), were also tested for stress–strain measurements; the resulting data are given in Table 7 while stress-strain curves are shown in Figure 9. As a general observation, a similar trend to that seen for the aforementioned specimens (PE-$20_{E/Ni1}$, PE-$30_{E/Ni1}$, PE-$40_{E/Ni1}$ and PE-$50_{E/Ni1}$) was observed with the properties dependent on the branching architectures and crystallinity. However, the comparatively higher molecular weight polyethylene showed better mechanical properties for these samples. For instance, both the ultimate tensile strength and maximum elongation at break for PE-$30_{M/Ni1}$ (M_w = 6.4 × 10^5 g mol^{-1}) are slightly higher than that seen for PE-$30_{E/Ni1}$ (M_w = 5 × 10^5 g mol^{-1}). Interestingly, the branching content of PE-$40_{M/Ni1}$ is less when compared to the PE-$40_{E/Ni1}$ specimen (142 *vs.* 167 per 1000 carbons, respectively), but the ultimate stress and maximum elongation at break are greater for PE-$40_{M/Ni1}$ over PE-$40_{E/Ni1}$. It would appear the higher molecular weight of the PE-$40_{M/Ni1}$ is the decisive factor on the elastomeric properties in this case.

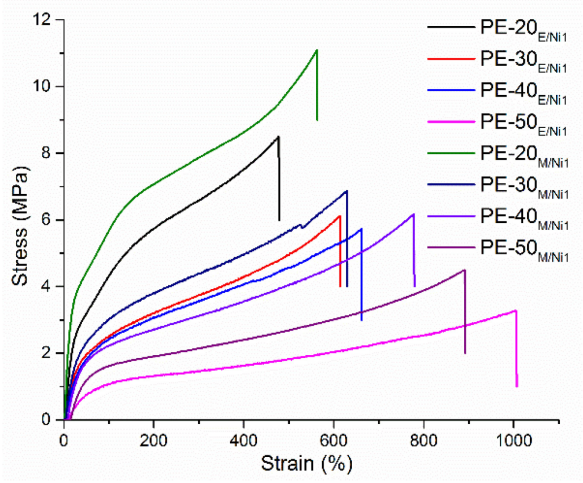

Figure 9. Stress–strain curves for PE-$20_{E/Ni1}$ – PE-$50_{E/Ni1}$ and PE-$20_{M/Ni1}$ – PE-$50_{M/Ni1}$; the vertical line represents the breakage point

Thirdly, to explore in more detail the effect of increased molecular weight on the mechanical properties, three samples of ultra-high molecular weight polymer designated PE-$30_{M/Ni3}$ (M_w = 3.1 × 10^6 g mol^{-1}), PE-$30_{M/Ni4}$ (M_w = 1.6 × 10^6 g mol^{-1}) and PE-$30_{M/Ni5}$ (M_w = 2.0 × 10^6 g mol^{-1}) were tested by stress-strain measurements; the resulting data are listed in Table 7 and stress-strain curves depicted in Figure 10. Significantly, the

Table 7. Selected properties of PE-$20_{E/Ni1}$ – PE-$50_{E/Ni1}$, PE-$20_{M/Ni1}$ – PE-$50_{M/Ni1}$ along with PE-$30_{M/Ni3}$, PE-$30_{M/Ni4}$ and PE-$30_{M/Ni5}$

Sample	T (°C)	T_m[a] (°C)	M_w[b]	Branches[c]/1000 C's	X_c[a] (%)	Stress[d] (MPa)	Strain[d] (%)
PE-$20_{E/Ni1}$	20	87.1	5.0	123	11.5	8.52	477.2
PE-$30_{E/Ni1}$	30	52.5	5.0	138	10.2	6.11	612.0
PE-$40_{E/Ni1}$	40	51.2	2.3	167	8.9	5.74	661.6
PE-$50_{E/Ni1}$	50	29.1	1.0	178	5.6	3.28	1002.0
PE-$20_{M/Ni1}$	20	94.6	5.4	159	14.5	11.92	562.1
PE-$30_{M/Ni1}$	30	63.2	6.4	173	8.08	6.88	630.0
PE-$40_{M/Ni1}$	40	53.9	5.0	142	4.0	6.17	778.9
PE-$50_{M/Ni1}$	50	47.0	3.1	200	2.8	4.51	892.23
PE-$30_{M/Ni3}$	30	53.4	30.8	178	10.7	13.22	843.9
PE-$30_{M/Ni4}$	30	59.0	15.7	156	13.8	8.95	801.1
PE-$30_{M/Ni5}$	30	63.1	19.8	165	11.1	11.84	817.2

[a] Determined by DSC, $X_c = \Delta H_f(T_m)/\Delta H°_f(T°_m)$, $\Delta H°_f(T°_m)$ = 248.3 J g^{-1}.[28] [b] M_w: x 10^5 g mol^{-1}, determined by GPC. [c] Determined by FT-IR.[29] [d] Determined using a universal tester.

ultra-high-molecular weight polyethylene showed better mechanical properties including ultimate tensile strength and maximum elongation at break. In comparison with PE-$30_{M/Ni1}$, the ultimate tensile strength significantly increased from 6.88 MPa to as high as 13.22 MPa for PE-$30_{M/Ni3}$ with the corresponding elongation break increasing from 630 to 843.9%. These changes are in agreement with this high molecular weight polyethylene sample showing better elastomeric properties.[9] Likewise, PE-$30_{M/Ni4}$ and PE-$30_{M/Ni5}$ also displayed superior properties when compared with PE-$30_{M/Ni1}$ or PE-$30_{E/Ni1}$.

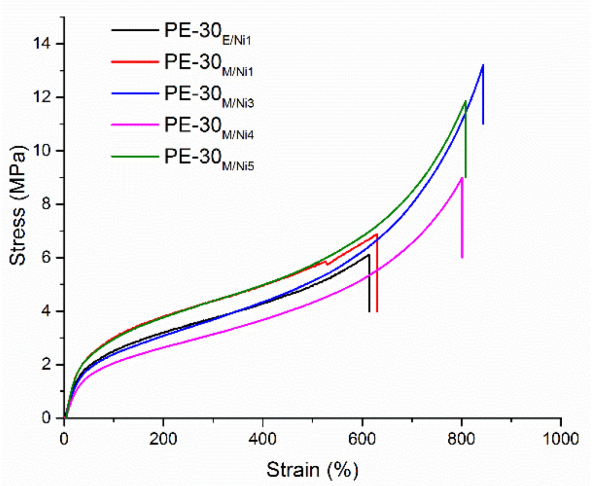

Figure 10. Stress–strain curves for PE-$30_{E/Ni1}$, PE-$30_{M/Ni1}$, PE-$30_{M/Ni3}$, PE-$30_{M/Ni4}$ PE-$30_{M/Ni5}$; the vertical line represents the breakage point

In order to assess further the elastomeric properties, the stress-strain recovery tests were performed by dynamic mechanical analysis (DMA) on firstly the lower molecular weight samples, namely PE-$30_{E/Ni1}$, PE-$40_{E/Ni1}$ and PE-$50_{E/Ni1}$; the results are shown in Figure 11. Typically, these tests were performed at -10 and 30 °C and each cycle was repeated up to ten times. After the first cycle, where the residual deformation gradually increases, all the materials exhibit a virtually constant level of recovery. This behavior is typical for thermoplastic elastomers and can be ascribed to the alignment of the polymer microstructure. After an initial change in morphology, a largely constant structure is adopted and hysteresis is observed. As the temperature of the stress-strain recovery tests increases from -10 °C to 30 °C, the elastic recovery of PE-$30_{E/Ni1}$ was improved from 50 to 56%. Likewise, the elastic recovery of PE-$40_{E/Ni1}$ increased from 65 to 68% and the elastic recovery of PE-$50_{E/Ni1}$ increased from 73 to 87%. The specimen of PE-$50_{E/Ni1}$ displayed the best elastic recovery and even after twenty cycles at 30 °C, an almost constant level of elastic recovery was observed (up to 81%, Figure S5). This suggested that the high branching content of these polyethylenes leads to high physical crosslinks which are a characteristic of typical thermoplastic elastomers.

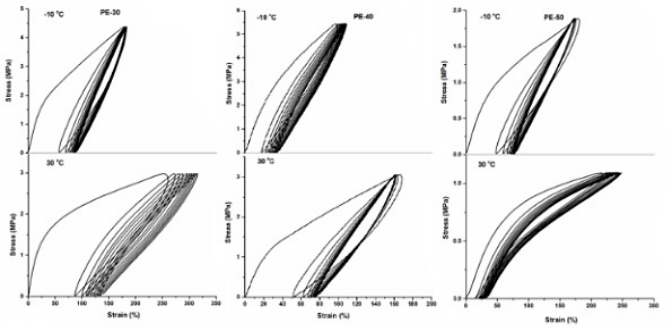

Figure 11. Stress–strain recovery tests for PE-$30_{E/Ni1}$, PE-$40_{E/Ni1}$ and PE-$50_{E/Ni1}$ at -10 and 30 °C.

Stress-strain recovery tests have also been performed on the ultra-high molecular weight samples, PE-$30_{M/Ni3}$ (M_w = 30.8 × 10^5 g mol^{-1}), PE-$30_{M/Ni4}$ (15.7 × 10^5 g mol^{-1}) and PE-$30_{M/Ni5}$ (19.8 × 10^5 g mol^{-1}) corresponding to the entries 1, 3-5 in Table 6. The hysteresis loops for just the one cycle for each sample are shown in Figure 12; the corresponding loop for PE-30_{MNi1} (M_w = 6.4 × 10^5 g mol^{-1}) is also presented for comparative purposes (the data for all ten cycles are given in Figure S6). In general, the elastic recovery of all three samples improves with increased molecular weight of the polyethylene. For example, the elastic recovery of PE-$30_{M/Ni3}$ was observed as 69% after 10 cycles of the test which is a significant

improvement on 50% for PE-30$_{M/Ni1}$. Likewise, the elastic recovery of PE-30$_{M/Ni4}$ and PE-30$_{M/Ni5}$ was superior with values of 55 and 58%, respectively.

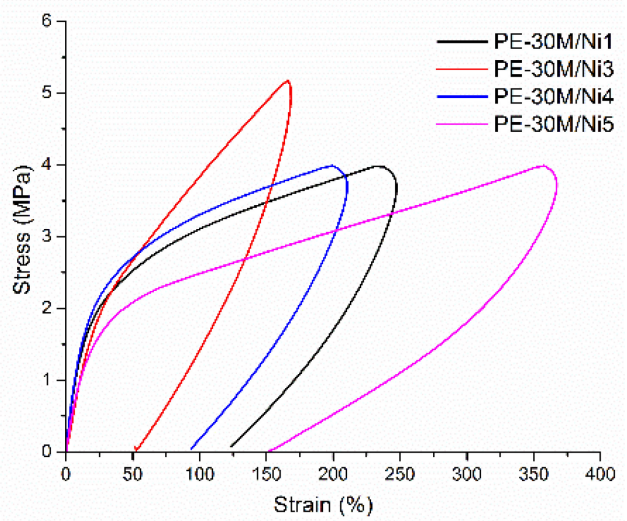

Figure 12. Comparative stress–strain hysteresis loops for PE-30$_{MNi1}$ (M_w = 6.4 × 10^5 g mole^{-1}), PE-30$_{M/Ni3}$ (M_w = 30.8 × 10^5 g mole^{-1}), PE-30$_{M/Ni4}$ (M_w = 15.7 × 10^5 g mole^{-1}) and PE-30$_{M/Ni5}$ (M_w = 19.8 × 10^5 g mole^{-1}) at 30 °C; for clarity purposes only one cycle is shown

For purposes of comparison, sample PE-30$_{M/Ni3}$ has been set against selected commercial polymers including linear low density polyethylene (LLDPE), low density polyethylene (LDPE), commercial polyolefin elastomer (CPOE) as well as homo-propylene (PP) elastomer; their crystallinity (X_c), stress (MPa), strain (%) and melting temperature (T_m) data are collected in Table S5.[9b,30] On examination of these data, it is evident that X_c of PE-30$_{M/Ni3}$ (10.7%) shows comparable values to those seen for CPOE (14%) and PP (10-16%) elastomers. By contrast LDPE and LLDPE, X_c can be anywhere between 40 – 80% while the T_m's between 106 – 125 °C (*c.f.* 53.4 °C for PE-30$_{M/Ni3}$). In terms of tensile stress, PE-30$_{M/Ni3}$ exhibited a value of 13.22 MPa which compares favourably to 13.62 MPa for CPOE while its elongation break, 843.9%, is also similar (845%).[30] In comparison with reported *a*PP-g-*i*PP graft copolymers,[31] PE-30$_{M/Ni3}$ displayed a lower elastic recovery (69% vs. 87%), while sample PE-50$_{E/Ni1}$ (Table 7) showed an identical value for the recovery at 250% strain after ten cycles (ε_b = 1002%). Furthermore, these elastomeric values are slightly higher than the TPE block copolymers reported by Coates *et al.* (strain at break 750% and elastic strain recovery 85%),[32] but comparable to the olefin block copolymers commercialized by Dow.[33]

Conclusions

Ten unsymmetrical 1,2-bis(arylimino)acenaphthene-nickel(II) halide complexes, each containing one N-2,6-dibenzhydryl-4-t-butyl-phenyl group but differing in the substitution pattern of the second N-aryl group or the type of halide have been successfully prepared and characterized by a range of techniques (*e.g.*, IR, ^{1}H NMR, XPE spectroscopy and X-ray diffraction). Upon activation with MMAO or Et_2AlCl, all the complexes exhibited exceptionally high activities at 30 °C for ethylene polymerization with the nickel bromides generally more active than the chlorides. What is more remarkable is the high molecular weight of the resultant polyethylenes which is particularly evident for the MMAO-promoted systems that, in most cases (**Ni3 - Ni10**), enters the ultra-high molecular weight window (i.e., > 1 x 10^6 g mol^{-1}). Furthermore, all the polymers are highly branched and display narrow molecular weight distributions (1.9 – 3.1), the latter characteristic of single-site catalysts. By comparison with structurally related catalysts it is clear that the presence of the *t*-butyl group on the *para*-position of the N-2,6-dibenzhydryl-4-t-butyl-phenyl group is having a dramatic effect on not only the activity but also the molecular weight. We attribute this observation to the electronic donating properties of this substituent and its effect on the relative rates of propagation and termination. Nevertheless, we cannot rule out a solubilising effect imparted by the t-butyl group that is improving catalyst activation. The microstructural and mechanical properties of these branched materials have been thoroughly investigated and reveal features characteristic of elastomers that improve with higher molecular weight. As a final comment, we view this work as highlighting a straightforward and single step route to high molecular weight thermoplastic elastomers which show great promise as potential alternatives to the those obtained by a co-polymerization approach.

Experimental section

General considerations

All manipulations involving air and/or moisture sensitive compounds were performed under an atmosphere of nitrogen using standard Schlenk techniques. Toluene was dried over sodium and distilled under nitrogen atmosphere prior to use. Methylaluminoxane (MAO, 1.46 M in toluene) and modified methylaluminoxane (MMAO, 1.93 M in heptane) were purchased from Akzo Nobel Corporation. Dimethylaluminum chloride (Me_2AlCl, 1.00 M in toluene) and diethylaluminum chloride (Et_2AlCl, 1.17 M in toluene) were supplied from Acros Chemical. High-purity ethylene was purchased from Beijing Yanshan Petrochemical Company and used as received. Other reagents were purchased from Aldrich, Acros or local suppliers. 2,6-Dibenzhydryl-4-(*t*-butyl)aniline was prepared using the literature route.[16] ^{1}H and ^{13}C NMR spectroscopic measurements for the organic compounds as well as the nickel complexes were performed on a Bruker DMX 400 MHz instrument at room temperature. Chemical shifts are measured in ppm for the ^{1}H and ^{13}C NMR spectra and are relative to TMS as an internal standard. Elemental analyses were conducted on a Flash EA 1112 microanalyzer. FT-IR spectra were carried out using a Perkin-Elmer System 2000 FT-IR spectrometer. Molecular weights (M_w) and molecular weight distributions (MWD) of the polyethylenes were determined using a PL-GPC220 instrument at 150 °C with 1,2,4-trichlorobenzene as the solvent. The melting temperatures of the polyethylenes were measured from the

second scanning run on a Perkin-Elmer TA-Q2000 DSC analyzer under a nitrogen atmosphere. In the procedure, a sample of about 4.0–6.0 mg was heated to 150 °C at a heating rate of 20 °C min^{-1} and kept for 5 min. at 150 °C to remove the thermal history and then cooled at a rate of 20 °C min^{-1} to -20 °C. The ^{13}C NMR spectra of the polyethylenes were recorded on a Bruker DMX 300 MHz instrument at 135 °C in deuterated 1,2-dichlorobenzene with TMS as an internal standard. The stress–strain curves were obtained using a universal tester (Instron 1122, UK). The stress–strain recovery tests at different temperatures were carried out using a dynamic mechanical analyzer (DMA800, TA) under controlled force mode.

Synthesis and characterization

2-(2,6-Dibenzhydryl-4-*t*-butylphenylimino)acenaphthylen-1-one (1)

To a solution of acenaphthylen-1,2-dione (3.64 g, 20 mmol) and *p*-toluenesulfonic acid (20 mol%) in ethanol (200 mL) was added a solution of 2,6-dibenzhydryl-4-(*t*-butyl)aniline (9.63 g, 20 mmol) in CH_2Cl_2 (40 mL) and the mixture stirred for 24 hours at room temperature. The resulting solution was concentrated on the rotary evaporator to give the crude product. Purification by silica gel column chromatography with petroleum ether/ethyl acetate (v/v = 50:1) as the eluent gave **1** as a red crystalline solid (9.04 g, 70%). Mp: 186-188 °C. FT-IR (KBr, cm^{-1}): 3059 (w), 2958 (w), 1727 (ν(C=O) m), 1657 (ν(C=N) m), 1598 (s), 1582 (s), 1492 (s), 1456 (m), 1332 (s), 1182 (w), 1028 (m), 911 (w), 825 (s). ^1H NMR (400 MHz, $CDCl_3$. TMS): δ 8.01 (t, *J* = 8.0 Hz, 2H, Ph-*H*), 7.71-7.68 (m, 2H, Ph-*H*), 7.24-7.21 (m, 4H, Ph-*H*), 7.16 (d, *J* = 6.8 Hz, 2H, Ph-*H*), 7.04-7.01 (m, 5H, Ph-*H*), 6.99 (s, 2H, Ph-*H*), 6.84 (d, *J* = 7.6 Hz, 4H, Ph-*H*), 6.59 (t, *J* = 7.2 Hz, 4H, Ph-*H*), 6.40 (t, *J* = 76 Hz, 2H, Ph-*H*), 6.00 (d, *J* = 7.2 Hz, 1H, Ph-*H*), 5.44 (s, 2H, 2 × C*H*), 1.16 (m, 9H, C(CH_3)$_3$). ^{13}C NMR (100MHz, $CDCl_3$. TMS): δ 189.7 (*C*=O), 162.3 (*C*=N), 146.6, 145.9, 143.1, 142.4, 141.9, 131.7, 131.1, 130.1, 129.9, 129.6, 129.3, 128.3, 128.0, 127.7, 127.4, 127.2, 127.1, 126.1, 125.4, 125.0, 123.8, 121.4, 52.4, 34.4, 31.4. Anal. Calcd for $C_{48}H_{39}NO$ (645.85): C, 89.27; H, 6.09; N, 2.17. Found: C, 89.10; H, 6.00; N, 2.14.

1-(2,6-Dibenzhydryl-4-*t*-butylphenylimino)-2-(2,6-dimethylphenylimino)acenaphthene (L1)

To a solution of 1 (1.0 g, 1.55 mmol) and *p*-toluenesulfonic acid (20 mol%) in dry toluene (50 mL) was added dropwise 2,6-dimethylaniline (0.20 g, 1.65 mmol) and the reaction mixture stirred and heated to reflux for 10 h using a Dean−Stark trap. After cooling to room temperature, the solvent was removed under reduced pressure. The residue was purified by alumina column chromatography using petroleum ether−ethyl acetate (v/v = 100:1) as the eluent affording **L1** as a deep yellow crystalline solid (0.37 g, 32%). Mp: 146-148 °C. FT-IR (KBr, cm^{-1}): 3026 (w), 2953 (w), 1659 (ν(C=N) m), 1631 (ν(C=N) m), 1593 (s), 1446 (s), 1361 (w), 1255 (w), 1110 (w), 1031 (m), 924 (s), 831 (s), 775 (m), 696 (s). ^1H NMR (400 MHz, $CDCl_3$, TMS): δ 7.70 (d, *J* = 8.0 Hz, 1H, Ph-*H*), 7.56 (d, *J* = 8.0 Hz, 1H, Ph-*H*), 7.24-7.21 (m, 5H, Ph-*H*), 7.18-7.15 (m, 4H, Ph-*H*), 7.09-7.07 (m, 5H, Ph-*H*), 6.98-6.91 (m, 7H, Ph-*H*), 6.59 (t, *J* = 8.0 Hz, 4H, Ph-*H*), 6.51 (d, *J* = 7.2 Hz, 1H, Ph-*H*), 6.40 (t, *J* = 7.2 Hz, 2H, Ph-*H*), 5.95 (d, *J* = 7.2 Hz, 1H, Ph-*H*), 5.63 (s, 2H, 2 × C*H*), 2.21 (s, 6H, 2 × CH_3), 1.17 (m, 9H, C(CH_3)$_3$). ^{13}C NMR (100 MHz, $CDCl_3$. TMS): δ 163.4 (*C*=N), 161.3 (*C*=N), 149.3, 146.7, 146.0, 143.5, 142.0, 139.9, 131.6, 129.8, 129.8, 129.5, 128.9, 128.7, 128.6, 128.3, 128.0, 127.9, 127.6, 127.4, 126.9, 126.0, 125.3, 125.1, 124.8, 124.1, 123.6, 121.6, 52.5, 34.4, 31.5, 14.1. Anal. Calcd for $C_{56}H_{48}N_2$ (749.01): C, 89.80; H, 6.46; N, 3.74. Found: C, 89.71; H, 6.41; N, 2.50.

1-(2,6-Dibenzhydryl-4-*t*-butylphenylimino)-2-(2,6-diethylphenylimino)acenaphthene (L2)

Using a similar procedure and molar ratios of reactants to that described for **L1**, **L2** was afforded **L2** as a deep yellow solid (0.42 g, 35%). Mp: 197-199 °C. FT-IR (KBr, cm^{-1}): 3026 (w), 2959 (w), 1659 (ν(C=N) m), 1632 (ν(C=N) m), 1593 (m), 1447 (s), 1361 (w), 1257 (m), 1111 (m), 1073 (m), 923 (s), 777 (w), 830 (m), 695 (s). ^1H NMR (400 MHz, $CDCl_3$, TMS): δ 7.68 (d, *J* = 8.0 Hz, 1H), 7.52 (d, *J* = 8.0 Hz, 1H), 7.25-7.14 (m, 10H), 7.08 (d, *J* = 7.6 Hz, 4H), 6.99 (s, 2H), 6.92-6.88 (m, 5H), 6.57 (t, *J* = 7.6 Hz, 4H), 6.50 (d, *J* = 7.2 Hz, 1H), 6.39 (d, *J* = 7.6 Hz, 2H), 5.86 (d, *J* = 8.0 Hz, 1H), 5.64 (s, 2H), 2.7-2.65 (m, 2H), 2.54-2.49 (m, 2H), 1.18-1.15 (m, 15H). ^{13}C NMR (100 MHz, $CDCl_3$, TMS): δ 163.5, 161.6, 148.4, 146.8, 146.0, 143.7, 142.0, 139.9, 131.6, 130.7, 129.7, 129.5, 128.9, 128.6, 128.5, 127.9, 127.7, 127.6, 127.1, 126.9, 126.1, 126.0, 125.4, 125.2, 124.1, 124.0, 122.2, 52.4, 34.4, 31.5, 24.4, 14.1. Anal. Calcd for $C_{58}H_{52}N_2$ (777.07): C, 89.65; H, 6.75; N, 3.61. Found: C, 89.71; H, 6.97; N, 3.63.

1-(2,6-Dibenzhydryl-4-*t*-butylphenylimino)-2-(2,6-diisopropylphenylimino)acenaphthene (L3)

Using a similar procedure and molar ratios of reactants to that described for **L1**, **L3** was afforded as a deep yellow solid (0.25 g, 28%). Mp: 211-213 °C. FT-IR (KBr, cm^{-1}): 3027 (w), 2959 (w) 1657 (ν(C=N) m), 1635 (ν(C=N) m), 1594 (m), 1453 (s), 1361 (m), 1254 (m), 1110 (w), 1075 (w), 923 (m), 829 (w), 780 (w), 695 (s). ^1H NMR (400 MHz, $CDCl_3$, TMS): δ 7.66 (d, *J* = 8.4 Hz, 1H), 7.48 (d, *J* = 8.0 Hz, 1H), 7.30-7.15 (m, 10H), 7.08 (d, *J* = 7.6 Hz, 4H), 7.00 (s, 2H), 6.90 (d, *J* = 7.2 Hz, 4H), 6.85 (t, *J* = 8.0 Hz, 1H), 6.55 (t, *J* = 7.6 Hz, 4H), 6.43 (d, *J* = 7.2 Hz, 1H), 6.37 (t, *J* = 7.6 Hz, 2H), 5.78 (d, *J* = 7.2 Hz, 1H), 5.65 (s, 2H), 3.17-312 (m, 2H), 1.28 (d, *J* = 6.8 Hz, 6H), 1.18 (s, 9H), 1.01 (d, *J* = 6.8 Hz, 6H). ^{13}C NMR (100 MHz, $CDCl_3$, TMS): δ 163.6, 162.0, 147.1, 146.8, 146.0, 143.8, 141.9, 140.0, 135.7, 131.6, 129.7, 129.5, 128.7, 128.5, 127.9, 127.7, 127.6, 126.9, 126.8, 125.9, 125.4, 125.2, 124.4, 124.2, 123.5, 122.8, 52.3, 34.4, 31.4, 28.4, 24.1, 23.7. Anal. Calcd for $C_{60}H_{56}N_2$ (805.12): C, 89.51; H, 7.01; N, 3.48. Found: C, 89.39; H, 7.43; N, 3.18.

1-(2,6-Dibenzhydryl-4-*t*-butylphenylimino)-2-(mesitylimino)acenaphthene (L4)

Using a similar procedure and molar ratios of reactants to that described for **L1**, **L4** was afforded as a deep yellow solid (0.47 g, 40%). Mp: 138-140 °C. FT-IR (KBr, cm^{-1}): 3028 (w), 2957 (w), 1666 (ν(C=N) m), 1640 (ν(C=N) m), 1595 (m), 1447 (m), 1361 (w), 1269 (m), 1154 (w), 1076 (w), 923 (m), 823 (w), 730 (s), 697 (s). ^1H NMR (400 MHz, $CDCl_3$, TMS): δ 7.70 (d, *J* = 7.2 Hz, 1H), 7.56 (d, *J* = 8.0 Hz, 1H), 7.27-7.21 (m, 6H), 7.16 (t, *J* = 7.2 Hz, 2H), 7.08 (d, *J* = 7.6 Hz, 4H), 6.97 (d, *J* = 4.8 Hz, 4H), 6.92 (s, 2H), 6.90 (s, 2H), 6.60-6.56 (m, 5H), 6.40 (t, *J* = 7.2 Hz, 2H), 5.94

(d, *J* = 7.2 Hz, 1H), 5.62 (s, 2H), 2.38 (s, 3H), 2.17 (s, 6H), 1.17 (s, 9H). ^{13}C NMR (100 MHz, $CDCl_3$, TMS): δ 163.4, 161.5, 146.8, 145.9, 143.4, 142.0, 139.9, 132.8, 131.5, 129.8, 129.4, 128.9, 128.7, 128.4, 127.9, 127.8, 127.6, 127.3, 126.8, 126.0, 125.3, 125.1, 124.6, 124.0, 121.6, 53.3, 52.4, 34.4, 31.4, 18.0, 14.0. Anal. Calcd for $C_{57}H_{50}N_2$ (763.04): C, 89.72; H, 6.61; N, 3.67. Found: C, 89.51; H, 6.63; N, 3.56.

1-(2,6-Dibenzhydryl-4-*t*-butylphenylimino)-2-(2,6-diethyl-4-methylphenylimino)acenaphthene (L5)

Using a similar procedure and molar ratios of reactants to that described for **L1**, **L5** was afforded as a deep yellow solid (0.52 g, 42%). Mp: 186-188 °C. FT-IR (KBr, cm^{-1}): 3028 (w), 2960 (w), 1667 (ν(C=N) m), 1641 (ν(C=N) m), 1596 (m), 1448 (m), 1361 (w), 1268 (m), 1182 (w), 1076 (w), 919 (m), 829 (w), 732 (s), 698 (s). ^{1}H NMR (400 MHz, $CDCl_3$, TMS): δ 7.67 (d, *J* = 8.4 Hz, 1H), 7.52 (d, *J* = 8.4 Hz, 1H), 7.25-7.21 (m, 6H), 7.17 (d, *J* = 7.2 Hz, 2H), 7.08 (d, *J* = 7.2 Hz, 4H), 7.00 (s, 2H), 6.99 (s, 2H), 6.92 (s, 2H), 6.90 (s, 2H), 6.57 (t, *J* = 6.8 Hz, 5H), 6.38 (t, *J* = 7.2 Hz, 2H), 5.85 (d, *J* = 7.2 Hz, 1H), 5.63 (s, 2H), 2.68-2.59 (m, 2H), 2.53-2.45 (m, 2H), 2.42 (s, 3H), 1.18-1.12 (m, 15H). ^{13}C NMR (100 MHz, $CDCl_3$, TMS): δ 163.5, 161.7, 146.8, 145.9, 145.8, 143.6, 141.9, 139.9, 133.1, 131.4, 129.7, 129.4, 128.9, 128.6, 128.3, 127.9, 127.6, 127.6, 127.1, 126.8, 126.8, 125.9, 125.3, 125.1, 124.0, 122.2, 52.3, 34.4, 31.4, 24.4, 14.0, 13.9. Anal. Calcd for $C_{59}H_{54}N_2$ (791.10): C, 89.58; H, 6.88; N, 3.54. Found: C, 89.32; H, 7.01; N, 3.34.

1-(2,6-Dibenzhydryl-4-*t*-butylphenylimino)-2-(2,6-dimethylphenylimino)acenaphthene-nickel dibromide (Ni1)

To a solution of **L1** (0.150 g, 0.20 mmol) in dichloromethane (10 mL) was added (DME)$NiBr_2$ (0.062 g, 0.20 mmol) under a nitrogen atmosphere. The reaction mixture was stirred for 24 h at ambient temperature and excess diethyl ether was added to precipitate the product. The product was collected by filtration, washed with diethyl ether (3 × 5 mL) and then dried under reduced pressure to give **Ni1** as a deep red solid (0.164 g, 85%). FT-IR (KBr, cm^{-1}): 3026 (w), 2958 (w), 1648 (*ν*(C=N), w), 1622 (*ν*(C=N), m), 1583 (m), 1493 (m), 1445 (s), 1291 (m), 1242 (s), 1185 (m), 1078 (m), 1033 (s), 920 (m), 828 (m), 770 (s), 699 (s). ^{1}H NMR (400 MHz, CD_2Cl_2, TMS): δ -16.62 (s, 1H, Ar–H_p), 3.71 (s, 9H, –C(CH_3)$_3$), 4.80 (s, 1H, An–*H*), 5.13 (s, 3H, Ar–*H*), 5.50 (s, 5H, Ar–*H*), 6.07 (s, 1H, An–*H*), 7.03-7.33 (m, 8H, Ar–*H*), 8.31 (s, 4H, Ar–*H*), 11.94 (broad, 1.3H, Ar–C*H*(Ph)$_2$), 16.01 (s, 1H, An–*H*), 16.81 (s, 1H, An–*H*), 20.44 (s, 1H, An–*H*), 23.16 (s, 2H, Ar–*H*), 25.14 (s, 1H, An–*H*), 26.27 (s, 2H, Ar–*H*), 29.39 (s, 6H, 2 × CH_3). Anal. Calcd for $C_{56}H_{48}Br_2N_2Ni$ (967.52): C, 69.52; H, 5.00; N, 2.90. Found: C, 69.71; H, 5.25; N, 2.95.

1-(2,6-Dibenzhydryl-4-*t*-butylphenylimino)-2-(2,6-diethylphenylimino)acenaphthene-nickel dibromide (Ni2)

Ni2 was prepared using a similar procedure and molar ratios to that described for **Ni1** affording a deep red solid (0.173 g, 87%). FT-IR (KBr, cm^{-1}): 3024 (w), 2958 (w), 1650 (*ν*(C=N), w), 1624 (*ν*(C=N), m), 1583 (m), 1494 (m), 1444 (s), 1292 (m), 1262 (s), 1187 (m), 1076 (m), 1029 (s), 943 (m), 823 (m), 767 (s), 699 (s). ^{1}H NMR (400 MHz, CD_2Cl_2, TMS): δ -16.28 (s, 1H, Ar–H_p), 0.73 (s, 6H, 2 × CH_3), 3.71 (s, 9H, –C(CH_3)$_3$), 4.81 (s, 1H, An–*H*), 5.01 (s, 1H, Ar–*H*), 5.16 (s, 3H, Ar–*H*), 5.58 (s, 5H, Ar–*H*), 6.05 (s, 1H, An–*H*), 7.01-7.30 (m, 7H, Ar–*H*), 8.28 (s, 4H, Ar–*H*), 11.75 (s, 1.25H, Ar–C*H*(Ph)$_2$), 16.02 (s, 1H, An–*H*), 16.75 (s, 1H, An–*H*), 20.45 (s, 1H, An–*H*), 23.18 (s, 2H, Ar–*H*), 25.23 (s, 1H, An–*H*), 25.94 (s, 2H, Ar–*H*), 26.95 (s, 2H, –CH_2), 28.89 (s, 2H, –CH_2). Anal. Calcd for $C_{58}H_{52}Br_2N_2Ni$ (995.57): C, 69.97; H, 5.26; N, 2.81. Found: C, 69.51; H, 5.29; N, 2.77.

1-(2,6-Dibenzhydryl-4-*t*-butylphenylimino)-2-(2,6-diisopropylphenylimino)acenaphthene-nickel dibromide (Ni3)

Ni3 was prepared using a similar procedure and molar ratios to that described for **Ni1** affording a deep red solid (0.166 g, 81%). FT-IR (KBr, cm^{-1}): 3022 (w), 2968 (w), 1638 (*ν*(C=N), w), 1616 (*ν*(C=N), m), 1577 (m), 1494 (m), 1447 (s), 1292 (m), 1259 (w), 1181 (m), 1075 (w), 1027 (s), 938 (m), 844 (w), 808 (s). ^{1}H NMR (400MHz, CD_2Cl_2, TMS): δ -15.77 (s, 1H, Ar–H_p), 1.67 (s, 6H, 2 × CH_3), 1.84 (s, 6H, 2 × CH_3), 3.85 (s, 9H, –C(CH_3)$_3$), 4.88 (s, 1H: An–*H*), 5.25 (s, 5H, Ar–*H*), 5.57 (s, 1H, An–*H*), 5.78 (s, 3H, Ar–*H*), 7.02 (s, 3H, Ar–*H*), 7.24 (5H, Ar–*H*), 8.24 (s, 4H, Ar–*H*), 12.51 (broad, 1.28H, Ar–C*H*(Ph)$_2$), 16.24 (s, 1H, An–*H*), 17.25 (s, 1H, An–*H*), 21.31 (s, 1H, An–*H*), 23.80 (s, 2H, Ar–*H*), 25.58 (s, 1H: An–*H;* 2H*:* Ar–*H*). Anal. Calcd for $C_{60}H_{56}Br_2N_2Ni$ (1023.62): C, 70.40; H, 5.51; N, 2.74. Found: C, 70.23; H, 5.94; N, 2.62.

1-(2,6-Dibenzhydryl-4-*t*-butylphenylimino)-2-(2,4,6-mesitylimino)acenaphthene-nickel dibromide (Ni4)

Ni4 was prepared using a similar procedure and molar ratios to that described for **Ni1** affording a deep red solid (0.169 g, 86%). FT-IR (KBr, cm^{-1}): 3027 (w), 2961 (w), 1648 (*ν*(C=N), w), 1621 (*ν*(C=N), m), 1583 (m), 1492 (m), 1360 (w), 1292 (m), 1262 (w), 1183 (m), 1079 (w), 1031 (s), 917 (w), 864 (m), 828 (s). ^{1}H NMR (400MHz, CD_2Cl_2, TMS): δ 3.69 (s, 9H, –C(CH_3)$_3$), 4.75 (s, 1H, An–*H*), 5.13 (s, 6H, Ar–*H*), 5.56 (s, 4H, Ar–*H*), 6.17 (s, 1H, An–*H*), 7.07 (s, 2H, Ar–*H*), 7.35 (s, 4H, Ar–*H*), 8.37 (s, 4H, Ar–*H*), 11.75 (broad, 1.19H, Ar–C*H*(Ph)$_2$), 15.99 (s, 1H, An–*H*), 16.75 (s, 1H, An–*H*), 20.19 (s, 1H, An–*H*), 23.10 (s, 2H, Ar–*H*), 25.67 (s, 1H, An–*H*), 25.93 (s, 2H, Ar–*H*), 29.43 (s, 6H, 2 × CH_3), 34.90 (s, 3H, –CH_3). Anal. Calcd for $C_{57}H_{50}Br_2N_2Ni$ (981.54): C, 69.75; H, 5.13; N, 2.85. Found: C, 69.61; H, 5.04; N, 2.70.

1-(2,6-Dibenzhydryl-4-*t*-butylphenylimino)-2-(2,6-diethyl-4-methylphenylimino)acenaphthene-nickel dibromide (Ni5)

Ni5 was prepared using a similar procedure and molar ratios to that described for **Ni1** affording a deep red solid (0.178 g, 88%). FT-IR (KBr, cm^{-1}): 3025 (w), 2962 (w), 1651 (*ν*(C=N), w), 1622 (*ν*(C=N), m), 1583 (m), 1494 (m), 1452 (s), 1363 (w), 1293 (m), 1261 (w), 1186 (m), 1075 (w), 1048 (w), 1032 (m), 962 (w), 897 (m), 866 (s). ^{1}H NMR (400 MHz, CD_2Cl_2, TMS): δ 3.73 (s, 9H, –C(CH_3)$_3$), 4.77 (s, 1H, An–*H*), 5.16 (s, 3H, Ar–*H*), 5.59 (s, 5H, Ar–*H*), 6.16 (s, 1H, An–*H*), 7.07 (s, 3H, Ar–*H*), 7.35 (s, 5H, Ar–*H*), 8.36 (s, 4H, Ar–*H*), 11.47 (broad, 1.27H, Ar–C*H*(Ph)$_2$), 16.10 (s, 1H, An–*H*), 16.79 (s, 1H, An–*H*), 20.34 (s, 1H, An–*H*), 23.28 (s, 2H, Ar–*H*), 25.76 (s, 2H, An–*H*), 25.96 (s, 1H, Ar–*H*), 27.13 (s, 2H, CH_2), 28.98 (s, 2H, CH_2) 35.03 (s, 3H, –CH_3). Anal. Calcd for $C_{59}H_{54}Br_2N_2Ni$ (1009.60): C, 70.19; H, 5.39; N, 2.77. Found: C, 70.03; H, 5.42; N, 2.75.

1-(2,6-Dibenzhydryl-4-*t*-butylphenylimino)-2-(2,6-dimethylphenylimino)acenaphthene-nickel dichloride (Ni6)

To a solution of **L1** (0.150 g, 0.20 mmol) in dichloromethane/ethanol (5/5 mL) was added $NiCl_2·6H_2O$ (0.047 g, 0.20 mmol) under a nitrogen atmosphere. The reaction mixture was stirred for 24 h at ambient temperature and then excess diethyl ether was added to precipitate the product. The product was collected by filtration, washed with diethyl ether (3 × 5 mL) and then dried under reduced pressure to give **Ni6** as a dark orange solid (0.155 g, 88%). FT-IR (KBr, cm^{-1}): 3020 (w), 2961 (s), 1652 (*ν*(C=N), w), 1624 (*ν*(C=N), m), 1584 (m), 1491 (w), 1445 (m), 1291 (w), 1222 (w), 1118 (m), 1079 (m), 1034 (s), 920 (w), 829 (s), 772 (s), 744 (m). ^{1}H NMR (400 MHz, CD_2Cl_2, TMS): δ -14.83 (s, 1H, Ar–H_p), -0.80 (s, 3H, Ar–*H*), 4.50 (s, 9H, –C(CH_3)$_3$), 4.74-4.76 (m, 1H, An–*H*; 2H, Ar–*H*), 5.00 (s, 5H, Ar–*H*), 5.89 (s, 1H, An–*H*), 7.02-7.05 (m, 2H, Ar–*H*), 7.31 (s, 4H, Ar–*H*), 8.60 (s, 4H, Ar–*H*), 10.94 (broad, 1.39H, Ar–C*H*(Ph)$_2$), 15.96 (s, 1H, An–*H*), 16.72 (s, 1H, An–*H*), 21.15 (s, 1H, An–*H*), 24.79 (s, 2H, Ar–*H*), 25.42 (s, 1H, An–*H*), 27.58 (s, 2H, Ar–*H*), 27.98 (s, 6H, 2 × CH_3). Anal. Calcd for $C_{56}H_{48}Cl_2N_2Ni·H_2O$ (896.62): C, 75.02; H, 5.62; N, 3.12. Found: C, 75.28; H, 5.50; N, 2.98.

1-(2,6-Dibenzhydryl-4-*t*-butylphenylimino)-2-(2,6-diethylphenylimino)acenaphthene-nickel dichloride (Ni7)

Ni7 was prepared using a similar procedure and molar ratios to that described for **Ni6** affording a dark orange solid (0.156 g, 86%). FT-IR (KBr, cm^{-1}): 3236 (w), 2965 (s), 1653 (*ν*(C=N), w), 1628 (*ν*(C=N), m), 1586 (s), 1494 (s), 1444 (s), 1292 (m), 1264 (w), 1188 (s), 1077 (m), 1032 (m), 944 (w), 869 (w), 823 (m). ^{1}H NMR (400 MHz, CD_2Cl_2, TMS): δ -14.19 (s, 1H, Ar–H_p), -0.38 (s, 3H, Ar–*H*), 0.56 (s, 6H, 2 × CH_3), 4.51 (s, 9H, –C(CH_3)$_3$), 4.85 (s, 1H, An–*H*; 2H, Ar–*H*), 5.12 (s, 5H, Ar–*H*), 5.92 (s, 1H, An–*H*), 6.99-7.02 (m, 2H, Ar–*H*), 7.25 (s, 4H, Ar–*H*), 8.52 (s, 4H, Ar–*H*), 10.94 (broad, 0.6H, Ar–C*H*(Ph)$_2$), 15.92 (s,1H, An–*H*), 16.59 (s, 1H, An–*H*), 21.16 (s, 1H, An–*H*), 24.03 (s, 2H, CH_2), 24.70 (s, 2H, Ar–*H*), 25.30 (s, 1H, An–*H*), 26.76 (s, 2H, CH_2), 27.05 (s, 2H, Ar–*H*). Anal. Calcd for $C_{58}H_{52}Cl_2N_2Ni·H_2O$ (924.68): C, 75.34; H, 5.89; N, 3.03. Found: C, 75.13; H, 5.78; N, 3.04.

1-(2,6-Dibenzhydryl-4-*t*-butylphenylimino)-2-(2,6-diisopropylphenylimino)acenaphthene-nickel dichloride (Ni8)

Ni8 was prepared using a similar procedure and molar ratios to that described for **Ni6** affording a dark orange solid (0.151 g, 81%). FT-IR (KBr, cm^{-1}): 3368 (b), 2966 (m), 1646 (*ν*(C=N), w), 1620 (*ν*(C=N), m), 1582 (s), 1446 (m), 1362 (w), 1291 (m), 1261 (m), 1114 (s), 1076 (m), 1031 (s), 769 (m), 742 (s). ^{1}H NMR (400 MHz, CD_2Cl_2, TMS): δ -13.91 (s, 1H, Ar–H_p), -0.02 (s, 3H, Ar–*H*), 1.13 (s, 6H, 2 × CH_3), 1.55 (s, 6H, 2 × CH_3), 4.68 (s, 9H, –C(CH_3)$_3$), 4.88 (s, 1H, An–*H*; 2H, Ar–*H*), 5.29 (s, 5H, Ar–*H*), 5.55 (s, 1H, An–*H*), 6.98 (s, 2H, Ar–*H*), 7.20 (s, 4H, Ar–*H*), 8.47 (4H, Ar–*H*), 11.21 (broad, 1.41H, Ar–C*H*(Ph)$_2$), 16.16 (s, 1H, An–*H*), 17.09 (s, 1H, An–*H*), 22.06 (s, 1H, An–*H*), 25.45 (s, 2H, CH_2), 25.81 (s, 1H, An–*H*), 26.92 (s, 2H, Ar–*H*). Anal. Calcd for $C_{60}H_{56}Cl_2N_2Ni·H_2O$ (952.73): C, 75.64; H, 6.14; N, 2.94. Found: C, 76.13; H, 6.54; N, 2.89.

1-(2,6-Dibenzhydryl-4-*t*-butylphenylimino)-2-(2,4,6-mesitylimino)acenaphthene-nickel dichloride (Ni9)

Ni9 was prepared using a similar procedure and molar ratios to that described for **Ni6** affording a light orange solid (0.157 g, 88%). FT-IR (KBr, cm^{-1}): 3425 (b) 2970 (m), 1652 (*ν*(C=N), w), 1623 (*ν*(C=N), m), 1585 (s), 1521 (s), 1493 (m), 1438 (m), 1339 (s), 1289 (m), 1082 (m), 1032 (s), 912 (m), 822 (m), 771 (m), 699 (s). ^{1}H NMR (400 MHz, CD_2Cl_2, TMS): δ -0.87 (s, 3H, Ar–*H*), 4.46 (s, 9H, –C(CH_3)$_3$), 4.69 (s, 1H, An–*H*) 4.76 (s, 2H, Ar–*H*), 4.99 (s, 5H, Ar–*H*), 6.00 (s, 1H, An–*H*), 7.05 (s, 2H, Ar–*H*), 7.32 (s, 4H, Ar–*H*), 8.64 (s, 4H, Ar–*H*), 10.51 (broad, 1.31H, Ar–C*H*(Ph)$_2$), 15.93 (s, 1H, An–*H*), 16.66 (s, 1H, An–*H*), 20.85 (s, 1H, An–*H*), 24.67 (s, 2H, Ar–*H*), 25.97 (s, 1H, An–*H*), 27.2 2 (s, 2H, Ar–*H*), 28.00 (s, 6H, 2 × CH_3), 35.50 (s, 3H, CH_3). Anal. Calcd for $C_{57}H_{50}Cl_2N_2Ni·H_2O$ (910.65): C, 75.18; H, 5.76; N, 3.08 Found: C, 75.00; H, 5.65; N, 2.92.

1-(2,6-Dibenzhydryl-4-*t*-butylphenylimino)-2-(2,6-diethyl-4-methylphenylimino)acenaphthene-nickel dichloride (Ni10)

Ni10 was prepared using a similar procedure and molar ratios to that described for **Ni6** affording a light orange solid (0.155 g, 84%). FT-IR (KBr, cm^{-1}): 3237 (b) 2964 (m), 1655 (*ν*(C=N), w), 628 (*ν*(C=N), m), 1586 (s), 1494 (s), 1445 (s), 1291 (m), 1076 (w), 1035 (w), 945 (w), 867 (m), 826 (m), 769 (s). ^{1}H NMR (400 MHz, CD_2Cl_2, TMS): δ -0.50 (s, 3H, Ar–*H*), 0.59 (s, 6H, 2 × CH_3), 4.53 (s, 9H, –C(CH_3)$_3$), 4.79-4.82 (m, 1H, An–*H*; 2H, Ar–*H*), 5.07 (s, 5H, Ar–*H*), 5.94 (s, 1H, An–*H*), 7.03 (m, 2H, Ar–*H*), 7.28 (s, 4H, Ar–*H*), 8.61 (s, 4H, Ar–*H*), 10.52 (broad, 0.6H, Ar–C*H*(Ph)$_2$), 15.97 (s,1H, An–*H*), 16.60 (s, 1H, An–*H*), 21.07 (s, 1H, An–*H*), 24.33 (s, 2H, CH_2), 24.86 (s, 0.12H, Ar–*H*), 25.95 (s, 1H, An–*H*), 26.93 (s, 2H, CH_2; 2H, Ar–*H*), 35.28 (s, 3H, CH_3). Anal. Calcd for $C_{59}H_{54}Cl_2N_2Ni·H_2O$ (938.70): C, 75.49; H, 6.01; N, 2.98. Found: C, 75.53; H, 5.74; N, 3.33.

X-ray crystallographic studies

Single crystals of **Ni1**, **Ni2** and **Ni6** suitable for the X-ray determinations were grown by layering heptane (**Ni1** and **Ni2**) or by slow diffusion of diethyl ether (**Ni6**) onto their respective dichloromethane solutions at room temperature. X-ray determinations were performed on a Rigaku Saturn 724+ CCD with graphite-monochromatic Mo-K$_\alpha$ radiation (λ = 0.71073 Å) at 173(2) K, the cell parameters were obtained by global refinement of the positions of all collected reflections. Intensities were corrected for Lorentz and polarization effects and empirical absorption. The structure was solved by direct methods and refined by full matrix least squares on F^2. All hydrogen atoms were placed in calculated positions. Structure solution and refinement were performed by using the Olex2 1.2 package.[34] The disorder displayed by the *t*-butyl and one ethyl group in **Ni2** was also processed by the SHELXL-97 software. During the structure refinement, solvent was squeezed (**Ni2**) with PLATON software.[35] Details of the crystal data and structure refinements for **Ni1**, **Ni2** and **Ni6** are shown in Table S6.

X-ray Photoelectron Spectroscopy (XPS) Studies

X-ray photoelectron spectroscopy was performed on a Thermo Scientific ESCA Lab 250Xi system (USA) using 200 W monochromatic Al-Kα radiation (hν = 1486.6 eV) at low temperature (-50 °C) with a cooling nitrogen gas stream controlled by liquid nitrogen. The base pressure was about 3 × 10^{-10} mbar. The binding energies were calibrated by referring to the hydrocarbon C (1s) peak at 284.8 eV. The Ni (2p), N (1s)

and Br (3p) regions were recorded with a higher resolution (a pass energy of 30 eV).

Typical procedure for ethylene polymerization

The polymerization at 10 atm. ethylene pressure was performed in a stainless steel autoclave (250 mL) equipped with an ethylene pressure control system, a mechanical stirrer and a temperature controller. At the required reaction temperature, the complex (2.0 μmol) dissolved in toluene (30 mL) was injected into the autoclave, followed by the addition of more toluene (30 mL) for washing purposes. The required amount of co-catalyst (MAO, MMAO, Me_2AlCl, Et_2AlCl) and more toluene were then added successively to complete the volume to 100 mL. The autoclave was immediately pressurized with 10 atm. pressure of ethylene and the stirring commenced. After the required reaction time, the ethylene pressure was vented and the reaction quenched with 10% hydrochloric acid in ethanol. The polymer was collected and washed with ethanol and dried under reduced pressure at 50 °C and weighed.

Acknowledgments

This work was supported by the National Natural Science Foundation of China (Nos. 21374123 and U1362204) and the National Key Research and Development Program of China (2016YFB1100800). QM is grateful to the CAS-TWAS president's fellowship. GAS thanks the Chinese Academy of Sciences for a Visiting Fellowship.

References

1 W. A. Braunecker and K. Matyjaszewski, *Prog. Polym. Sci.*, 2007, **32**, 93.
2 M.; Akiba and A. S. Hashim, *Prog. Polym. Sci.*, 1997, **22**, 475.
3 B. Adhikari, D. De and S. Maiti, *Prog. Polym. Sci.*, 2000, **25**, 909.
4 (a) L. R. Kucera, M. R. Brei and R. F. Storey, *Polymer,* 2013, **54**, 3796; (b) E. Espinosa, B. Charleux, F. D'Agosto, C. Boisson, R. Tripathy, R. Faust and C. Soulie-Ziakovic, *Macromolecules*, 2013, **46**, 3417; (c) X. Xia, Z. Ye, S. Morgan and J. Lu, *Macromolecules*, 2010, **43**, 4889; (d) L. R. Hutchings, J. M. Dodds, D. Rees, S. M. Kimani, J. J. Wu and E. Smith, *Macromolecules,* 2009, **42**, 8675.
5 D. J. Arriola, E. M. Carnahan, P. D. Hustad, R. L. Kuhlman and T. T. Wenzel, *Science*, 2006, **312**, 714.
6 M. C. Baier, M. A. Zuideveld and S. Mecking, *Angew. Chem., Int. Ed*., 2014, **53**, 9722.
7 (a) L. K. Johnson, C. M. Killian and M. Brookhart, *J. Am. Chem. Soc.*, 1995, **117**, 6414; (b) C. M. Killian, D. J. Tempel, L. K. Johnson and M.Brookhart, *J. Am. Chem. Soc.*, 1996, **118**, 11664; (c) V. C. Gibson, C. Redshaw and G. A. Solan, *Chem. Rev.*, 2007, **107**, 1745; (d) W.-H. Sun, *Adv. Polym. Sci.*, 2013, **258**, 163; (d) C. M. Killian, L. K. Johnson and M. Brookhart, *Organometallics*, 1997, **16**, 2005; (e) D. H. Leung, J. W. Ziller and Z. Guan, *J. Am. Chem. Soc.,* 2008, **130**, 7538-7539.
8 (a) R. Gao, W.-H. Sun and C. Redshaw, *Catal. Sci. Technol.*, 2013, **3**, 1172; (b) Q. Xing, T. Zhao, Y. Qiao, L. Wang, C. Redshaw and W.-H. Sun, *RSC Adv*. 2013, **3**, 26184; (c) S. Wang, W. Zhao, X. Hao, B. Li, C. Redshaw, Y. Li and W.-H. Sun, *J. Organomet. Chem.*, 2013, **731**, 78; (d) F. Huang, Q. Xing, T. Liang, Z. Flisak, B. Ye, X. Hu, W. Yang and W.-H. Sun, *Dalton Trans.,* 2014, **43**, 16818; (e) S. Wang, W.-H. Sun and C. Redshaw, *J. Organomet. Chem.,* 2014, **751**, 717; (f) Z. Flisak and W.-H. Sun, *ACS Catal.,* 2015, **5**, 4713; (g) J. Ma, C. Feng, S. Wang, K.-Q. Zhao, W.-H. Sun, C. Redshaw and G. A. Solan, *Inorg. Chem. Front*., 2014, **1**, 14; (h) D. Jia, W. Zhang, W. Liu, L. Wang, C. Redshaw and W.-H. Sun, *Catal. Sci. Technol.,* 2013, **3**, 2737; (i) S. Song, T. Xiao, T. Liang, F. Wang, C. Redshaw and W.-H. Sun, *Catal. Sci. Technol.,* 2011, **1**, 69; (j) W.-H. Sun, S. Song, B. Li, C. Redshaw, X. Hao, Y.-S. Lib and F. Wang, *Dalton Trans*., 2012, **41**, 11999; (k) K. Song, W. Yang, B. Li, Q. Liu, C. Redshaw, Y. Li and W.-H. Sun, *Dalton Trans.*, 2013, **42**, 9166; (l) X. Wang, L. Fan, Y. Ma, C.-Y. Guo, G. A. Solan, Y. Sun and W.-H. Sun, *Polym. Chem.*, 2017, **8**, 2785.
9 (a) B. Rieger and C. Troll, *Macromolecules,* 2002, **35***,* 5742; (b) C. Cobzaru, S. Hild, A. Boger, C. Troll and B. Rieger, *Coord. Chem. Rev.*, 2006, **250**, 189; (c) U. Dietrich, M. Hackmann, B. Rieger, M. Klinga and M. Leskela, *J. Am. Chem. Soc.,* 1999, **121***,* 4348.
10 (a) H. Liu, W. Zhao, X. Hao, C. Redshaw, W. Huang and W.-H. Sun, *Organometallics,* 2011, **30**, 2418; (b) S. Kong, C.-Y. Guo, W. Yang, L. Wang, W.-H. Sun and R. Glaser, *J. Organomet. Chem.,* 2013, **725**, 37.
11 (a) D. P. Gates, S. A. Svejda, E. Oñate, C. M. Killian, L. K. Johnson, P. S. White and M. Brookhart, *Macromolecules,* 2000, **33**, 2320; (b) Z. Chen, K. E. Allen, P. S. White, O. Daugulis and M. Brookhart, *Organometallics,* 2016, **35**, 1756; (c) V. Katla, E. Yue, N. M. Rajendran, T. Liang and W.-H. Sun, *C. R. Chim.,* 2016, **19**, 604-613; (d) Z. Wang, Q. Liu, G. A. Solan and W.-H. Sun, *Coord. Chem. Rev.,* 2017*,* DOI: 10.1016/j.ccr.2017.06.003; (e) C. Wen, S. Yuan, Q. Shi, E. Yue, D. Liu and W.-H. Sun, *Organometallics,* 2014, **33**, 7223; (f) L. Fan, E. Yue, S. Du, C.-Y. Guo, X. Hao and W.-H. Sun, *RSC Adv.*, 2015, 5, 93274; (g) S. Yuan, E. Yue, C. Wen and W.-H. Sun, *RSC Adv.,* 2016, **6**, 7431; (h) X. Wang, L. Fan, Y. Yuan, S. Du, Y. Sun, G. A. Solan, C.-Y. Guo, and W.-H. Sun, *Dalton Trans.*, 2016, **45**, 18313; (i) S. Du, S. Kong, Q. Shi, J. Mao, C. Guo, J. Yi, T. Liang and W.-H. Sun, *Organometallics*, 2015, **34**, 582.
12 (a) Y. Chen, S. Du, C. Huang, G. A. Solan, X. Hao and W.-H. Sun, *J. Polym. Sci., Part A: Polym. Chem.,* 2017, **55**, 1971; (b) Y. Zeng, Q. Mahmood, X. Hao and W.-H. Sun, *J. Polym. Sci., Part A: Polym. Chem.*, 2017, **55**, 1910; (c) H. Liu, W. Zhao, J. Yu, W. Yang, X. Hao, C. Redshaw, L. Chen and W.-H. Sun, *Catal. Sci. Technol.,* 2012, **2**, 415; (d) L. Fan, S. Du, C.-Y. Guo, X. Hao and W.-H. Sun, *J. Polym. Sci., Part A: Polym. Chem.,* 2015, **53**, 1369; (e) Q. Mahmood, Y. Zeng, X. Wang, Y. Sun and W.-H. Sun, *Dalton Trans.,* 2017, **46**, 6934; (f) J. Yu, Y. Zeng, W. Huang, X. Hao and W.-H. Sun, *Dalton Trans.,* 2011, **40**, 8436; (g) Y. Zhang, C. Huang, X. Wang, Q. Mahmood, X. Hao, X. Hu, C.-Y. Guo, G. A. Solan and W.-H. Sun, *Polym. Chem*., 2017, **8**, 995; (h) J. Yu, X. Hu, Y. Zeng, L. Zhang, C. Ni, X. Hao and W.-H. Sun, *New J. Chem*., 2011, **35**, 178; (i) C. Huang, Y. Zeng, Z. Flisak, Z. Zhao, T. Liang and W.-H. Sun, *J. Polym. Sci., Part A: Polym. Chem.,* 2017, 55, 2071; (j) Y. Zeng, Q. Mahmood, T. Liang and W.-H. Sun, *J. Polym. Sci., Part A: Polym. Chem.,* 2017, **55**, DOI:10.1002/pola.28663.
13 J. L. Rhinehart, N. E. Mitchell and B. K. Long, *ACS Catal*., 2014, **4***,* 2501.
14 (a) T. Zhang, D. Guo, S. Jie, W.-H. Sun, T. Li and X. Yang, *J. Polym. Sci., Part A: Polym. Chem.*, 2004, **42**, 4765; (b) W. Yang, J. Yi and W.-H. Sun, *Macromol. Chem. Phys*., 2015, **216**, 1125.
15 C. Huang, Y. Zhang, T. Liang, Z. Zhao, X. Hu and W.-H. Sun, *New J. Chem.,* 2016, **40**, 9329.
16 S. Meiries, K. Speck, D. B. Cordes, A. M. Z. Slawin and S. P. Nolan, *Organometallics*, 2013, **32**, 330.
17 J. L. Rhinehart, L. A. Brown and B. K. Long, *J. Am. Chem. Soc*., 2013, **135**, 16316.

18 S. Du, Q. Xing, Z. Flisak, E. Yue, Y. Sun and W.-H. Sun, *Dalton Trans*., 2015, **44**, 12282.
19 B. R. McGarvey, *Inorg. Chem.*, 1995, **34**, 6000.
20 H. Gao, X. Liu, Y. Tang, J. Pan and Q. Wu, *Polym. Chem*., 2011, **2**, 1398.
21 (a) G. J. P. Britovsek, S. A. Cohen, V. C. Gibson and M. V. Meurs, *J. Am. Chem. Soc.,* 2004, **126**, 10701; (b) E. Yue, L. Zhang, Q. Xing, X.-P. Cao, X. Hao, C. Redshaw and W.-H. Sun, *Dalton Trans*., 2014, **43**, 423.
22 C. C. H. Atienza, C. Milsmann, E. Lobkovsky and P. J. Chirik, *Angew. Chem. Int. Ed.*, 2011, **50**, 8143.
23 W. Krauss and W. Gestrich, *Chem.-Technol*. 1977, **6**, 513.
24 F. Huang, Z. Sun, S. Du, E. Yue, J. Ba, X. Hu, T. Liang, G. B. Galland and W.-H. Sun, *Dalton Trans.,* 2015, **44**, 14281.
25 G. B. Galland, R. F. De Souza, R. S. Mauler and F. F. Nunes, *Macromolecules,* 1999, **32**, 1620.
26 B. Gabrielle, L. Guy, P.-A. Albouy, L. Vanel, D. R. Long and P.Sotta, *Macromolecules,* 2011, **44**, 7006.
27 Z. He, Y. Liang, W. Yang, H. Uchino, J. Yu, W.-H. Sun and C. C. Han, *Polymer*, 2015, **56**, 119.
28 Y. Kong and J. N. Hay, *Polymer,* 2002, **43**, 3873.
29 T. Usami and S. Takayama, *Polym. J.,* 1984, **16**, 731.
30 (a) S. Guo, H. Fan, Z. Bu, B-G. Li and S. Zhu, *Polymer,* 2015, **80**, 109; (b) P. S. Chum and K. W. Swogger, *Prog. Polym. Sci.*, 2008, **33**, 797.
31 K. S. O'Connor, A. Watts, T. Vaidya, A. M. LaPointe, M. A. Hillmyer and G. W. Coates, *Macromolecules* 2016, **49**, 6743.
32 J. M. Rose, F. Deplace, N. A. Lynd, Z. Wang, A. Hotta, E. B. Lobkovsky, E. J. Kramer and G. W. Coates, *Macromolecules* 2008, **41**, 9548.
33 W. Weng, A. H. Dekmezian, E. J. Markel and D. L. Peters, U.S. Patent 6, 2001, 184, 327.
34 Sheldrick, G. M. SHELXTL-97, Program for the Refinement of Crystal Structures; University of Göttingen, Göttingen, Germany, 1997.
35 L. Spek, *Acta Crystallogr., Sect. D: Biol. Crystallogr*., 2009, **65**, 148.